

# From Adsorption to Covalent Bonding: Apolipoprotein E Functionalization of Polymeric Nanoparticles for Drug Delivery Across the Blood–Brain Barrier

Natascha Hartl, Friederike Adams, and Olivia M. Merkel\*

The blood–brain barrier (BBB) is composed of brain endothelial cells, pericytes, and astrocytes, which build a tight cellular barrier. Therapeutic (macro)molecules are not able to transit through the BBB in their free form. This limitation is bypassed by apolipoprotein E (ApoE)-functionalized polymeric nanoparticles (NPs) that are able to transport drugs (e.g., dalargin, loperamide, doxorubicin, and nerve growth factor) across the BBB via low density lipoprotein (LDL) receptor-mediated transcytosis. Coating with polysorbate 80 or poloxamer 188 facilitates ApoE adsorption onto polymeric NPs enabling recognition by LDL receptors of brain endothelial cells. This effect is even enhanced when NPs are directly coated with ApoE without surfactant anchor. Similarly, covalent coupling of ApoE to NPs that bear reactive groups on their surface leads to significantly improved brain uptake while avoiding the use of surfactants. In this Progress Report several *in vitro* BBB models using brain endothelial cells or cocultures with astrocytes/pericytes/glioma cells are described, which provide insights regarding the ability of a drug delivery system to cross this barrier. In vivo models are described which simulate central nervous system-relevant diseases such as Alzheimer's or Parkinson's disease and cerebral cancer.

high molecular weight.<sup>[1]</sup> Furthermore, those few drugs that are capable of crossing the BBB can be actively transported back into the vasculature by efflux transporters.<sup>[2]</sup> Consequently, the delivery and release of drugs into the brain is a challenging topic that requires specific systems for drugs to transit the BBB. In the past, several approaches have been tested to transiently open or to passage this barrier. Intrathecal or intraventricular injection of drugs represents an invasive method, which has been used for chemotherapy with methotrexate or cytarabine/cortisol in patients with aggressive lymphoma or acute lymphatic leukemia.<sup>[3]</sup> With infusion of hyperosmotic solutions via the arteria carotis interna, a shrinkage of endothelial cells and opening of tight junctions is achieved.<sup>[4]</sup> This approach has clinically been used, but the unselective opening of the BBB was accompanied by the risk of edema formation.<sup>[5]</sup> Moreover, shear forces of microcurrents induced by applied focused


## 1. Introduction

According to the World Health Organization (WHO), approximately 20% of all humans suffer from damages of the central nervous system (CNS), such as depression, epilepsy, Parkinson's disease, dementia/Alzheimer's disease (AD), stroke, cerebral cancer or CNS-relevant metabolic diseases. Due to the strong protective function of the blood–brain barrier (BBB), the ability of therapeutic agents to reach their targets in the CNS is extremely limited. Less than 2% of small molecule drugs are able to cross this barrier with even lower numbers for macromolecules due to their

ultrasound in the area of treatment cause a local disruption of the BBB, which was shown by the group of Treat in animal trials.<sup>[6]</sup> Schinkel et al. showed that the CNS concentration of various drugs is significantly increased by blockage or knock-out of efflux transporters in the BBB.<sup>[7]</sup> However, these transporters are also blocked in other barriers of the body leading to altered pharmacokinetics of many endogenous and exogenous compounds. Due to unspecific side effects of the above described disrupting methods, the design of efficient noninvasive nanocarrier systems that can facilitate controlled and targeted drug delivery to the specific regions of the brain is the goal of many current research efforts, but is also a major challenge.<sup>[8]</sup> As a promising nanocarrier system, liposomes have been investigated initially for small molecule drug encapsulation and delivery. To achieve specific targeting of the brain endothelium the transport pathway of receptor-mediated transcytosis (RMT) was utilized with these systems after surface modification with target seeking ligands.<sup>[9]</sup> Ligand-decorated liposomes bind to specific receptors, are endocytosed and the liposomal content is transported across the BBB.<sup>[10]</sup> As ligands directed against transferrin receptors overexpressed on the BBB, i.e., transferrin receptor antibodies were coupled to liposomes.<sup>[9]</sup>

Also the low density lipoprotein-(LDL) receptor family, a group of cell surface receptors that transport several macromolecules into cells, is expressed in several different tissues

N. Hartl, Dr. F. Adams, Prof. O. M. Merkel  
Pharmaceutical Technology and Biopharmaceutics  
Department Pharmacy  
Ludwig-Maximilians-University  
Butenandtstr. 5-13, Munich 81377, Germany  
E-mail: olivia.merkel@lmu.de

 The ORCID identification number(s) for the author(s) of this article can be found under <https://doi.org/10.1002/adtp.202000092>

© 2020 The Authors. Published by WILEY-VCH Verlag GmbH & Co. KGaA, Weinheim. This is an open access article under the terms of the Creative Commons Attribution License, which permits use, distribution and reproduction in any medium, provided the original work is properly cited.

DOI: 10.1002/adtp.202000092

and can also be found in the brain.<sup>[11]</sup> These receptors play a crucial role in the homeostasis of triglycerides and cholesterol by mediating cellular uptake of apolipoprotein-containing lipoprotein particles.<sup>[12]</sup> An alternative to liposomes are polymeric nanoparticles (NPs), consisting of low-cost, stable, tailored and biodegradable materials, e.g., poly(lactic-co-glycolic acid) (PLGA) or poly(*n*-butylcyanoacrylate) (PBCA), making them advantageous over liposomes.<sup>[13]</sup> Up to date, there is a very urgent need to also use macromolecules as therapeutics for CNS diseases. Promising compounds are high molecular weight biologicals, e.g., antibodies for Alzheimer's disease and multiple sclerosis, enzymes for lysosomal storage diseases, or peptides for ischemic brain diseases.<sup>[14]</sup> Especially polymeric NP systems provide a promising delivery tool for embedding these macromolecules as well as small molecule drugs. The following progress report will focus on the latest developments in LDL receptor-mediated brain targeting with ApoE-functionalized polymeric NPs. Special emphasis is given on the different polymeric materials, encapsulated drugs, in vitro BBB models and in vivo setups simulating different CNS-relevant diseases.

## 2. Blood–Brain Barrier

### 2.1. Structure and Physiological Function of the Blood–Brain Barrier

The CNS is the most critical and sensitive organ in the human body and needs a regulated extracellular environment. Neurons, astrocytes, endothelial cells of the BBB, myocytes, pericytes, and extracellular matrix components form the neurovascular unit (NVU) that serves to maintain CNS homeostasis. The capillaries of the CNS have evolved to restrain the movement of molecules and cells between blood and the brain. The BBB is a highly regulated and efficient biological barrier between the peripheral circulation and the CNS. The BBB controls brain homeostasis as well as ion and molecule movement and protects the brain against metabolites, xenobiotics, pathogens, and a multitude of drugs. The cellular barrier of the BBB is composed of brain microvessel endothelial cells, pericytes, as a second line of defense, and astrocyte end feet, which tightly ensheath the vessel wall (**Figure 1**). Pericytes are known to have various functions in the CNS such as modulation of endothelial permeability, stabilization of microvessel walls by intimate contact to endothelial cells, supply of BBB-specific enzymes and phagocytotic activity. Astrocytes, solely or in combination with neurons, act as mediators in regulation of CNS microvascular permeability. Their end feet cover pericytes and endothelial cell walls, release trophic factors that are essential for the induction and maintenance of the BBB and are involved in water and ion balance regulation.<sup>[15]</sup> BBB endothelial cells differ from endothelial cells in the rest of the body by the absence of fenestration and presence of extremely tight junction complexes in the interendothelial space that includes tight junction proteins, adhesion junctions, junctional adhesion molecules, and accessory proteins. The presence of junction complexes and the lack of aqueous pathways between cells greatly restricts permeation of polar solutes through paracellular diffusional pathways from the blood plasma to the brain extracellular fluid.<sup>[16]</sup> The tight junctions consist of three integral membrane proteins, namely,

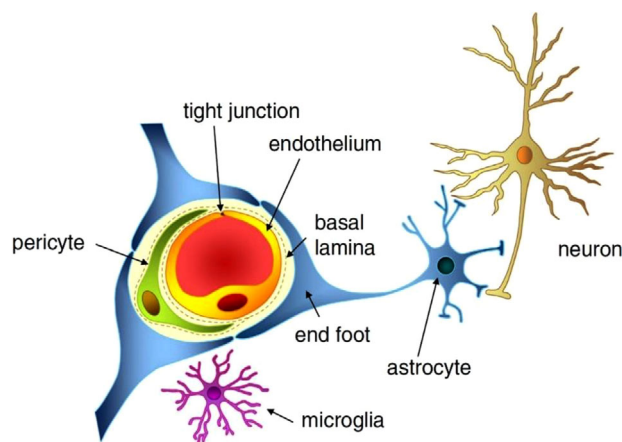


**Figure 1.** The neurovascular unit and structures that contribute to the BBB, i.e., endothelial cells, tight junctions, pericytes, and astrocytic end feet. Reproduced with permission.<sup>[117]</sup> Copyright 2013, John Wiley and Sons.

claudin, occludin, and junction adhesion molecules (JAM) and a number of cytoplasmic accessory proteins including zonula occludens proteins and cingulin.<sup>[15]</sup> Occludin appears to be a regulatory protein that can alter the paracellular permeability. JAM is involved in cell-to-cell adhesion and monocyte transmigration through BBB.<sup>[17]</sup> All described components are essential for the normal function and stability of the BBB.

### 2.2. Transport Routes across the BBB

Substances can cross the BBB via different pathways (**Figure 2**). The first route is paracellular transport, which involves passing in between the endothelial cells across the tight junctions. Through simple passive diffusion water and small water-soluble substances are capable of passing the BBB (**Figure 2A**). The second pathway is transcellular transport and occurs via diffusion of small lipophilic gases and some lipid-soluble compounds, such as alcohol and steroid hormones, from the endothelial cells into the brain stroma in a passive way (**Figure 2B**).<sup>[8]</sup> Larger and more hydrophilic nutrients and metabolites, that are essentially required by the nervous tissue, need to be taken up in an active way.<sup>[18]</sup> Therefore, specific transport mechanisms for these active pathways, i.e., carrier-, receptor-, and adsorptive-mediated transcytosis or efflux transporters, are embedded in the BBB to guarantee an adequate supply and export of these substances.<sup>[19]</sup> In case of carrier-mediated transcytosis (CMT), solutes such as glucose, amino acids or essential fatty acids bind to a transport protein, which is embedded in the membrane of the endothelium (**Figure 2C**). This interaction leads to a change in the carrier protein conformation, resulting in transport through the endothelial cell along or against a concentration gradient.<sup>[8]</sup> Specific efflux transporters, inserted predominantly in the apical membrane, act as extremely efficient efflux pumps and are capable of rapidly pumping back potentially toxic components into the blood stream (**Figure 2D**). These efflux transporters include members of the ATP-binding cassette (ABC) gene family, e.g., P-glycoprotein, multidrug resistance proteins (MRPs), and breast cancer resistance proteins (BCRP) that are highly overexpressed

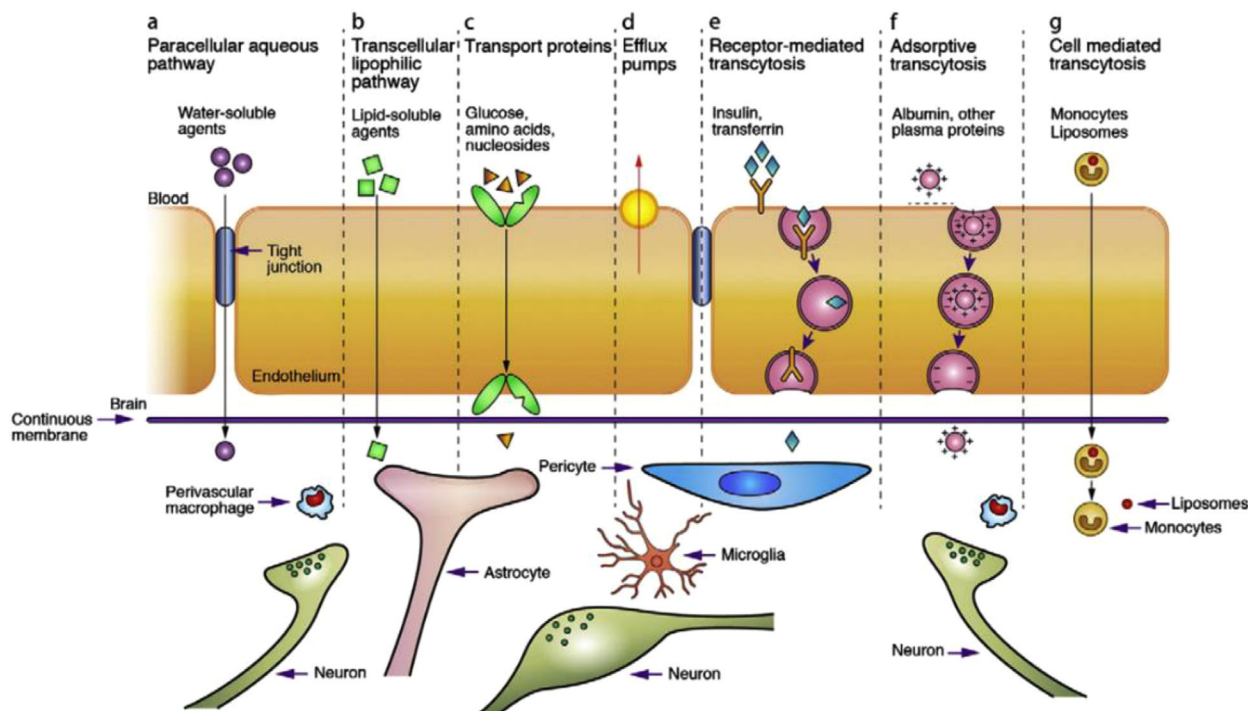


**Figure 2.** Different transport pathways to pass the BBB. Reproduced with permission.<sup>[8]</sup> Copyright 2012, Elsevier.

by endothelial cells of the BBB.<sup>[20]</sup> The vesicular mechanism that provides the main route for the entry of macromolecules, such as proteins, into the brain involve either receptor-mediated transcytosis (RMT) or adsorptive-mediated transcytosis (AMT). In RMT, binding of macromolecular ligands to specific receptors on the cell surface triggers endocytosis (Figure 2E). Receptors and their bound ligands form complexes that are internalized into the endothelial cells as pinocytotic vesicles. These vesicles move through the cytoplasm to the basolateral sides of the endothelial cells where they are exocytosed. Dissociation of the ligand–receptor complex presumably occurs during cellular transit or exocytosis.<sup>[21]</sup> So far, several receptors have been identified that can initiate RMT, e.g., insulin, epidermal growth factor, transferrin and LDL-related protein receptors.<sup>[22]</sup> AMT is induced by ligands bearing a positive charge, so that they can interact electrostatically with negatively charged cell surface binding sites and subsequently are absorbed and transcytosed (Figure 2F).<sup>[23]</sup> In both pathways, the degradative lysosomal compartment within the cell needs to be avoided to ensure entry of intact compounds to the brain.<sup>[24]</sup>

### 3. Apolipoprotein E and Its Associated Receptors

#### 3.1. Apolipoprotein E

Lipoproteins are biological carriers transporting both lipids and proteins systemically through the body. Lipoproteins, which consist of lipids and proteins, are classified based on the proportions of these two substances and their density into five main categories, namely chylomicrons, very low-density lipoproteins (VLDL), intermediate-density lipoproteins (IDL), LDL and

high-density lipoproteins (HDL).<sup>[11a]</sup> Lipoproteins are composed of an insoluble core of cholesteryl ester and triglycerides surrounded by a shell of amphiphilic phospholipids and specialized proteins called apolipoproteins (Apo).<sup>[25]</sup> Plasma lipoprotein metabolism is regulated and controlled by these specific apolipoprotein parts, as they are involved in the redistribution of lipids among cells and tissues, in the maintenance of the lipoprotein structures as well as in enzyme activation levels. The most common apolipoproteins are ApoE, ApoB, ApoA-I, ApoA-IV, ApoC-I, ApoC-II, and ApoC-III.<sup>[26]</sup> Apolipoprotein E (ApoE) is a component found in lipoprotein classes VLDL and chylomicrons. Therefore, the major function of ApoE is the transport of triglycerides and cholesterol from sites of synthesis or adsorption to sites of utilization (peripheral tissues) or excretion (liver).<sup>[27]</sup> ApoE-mediated lipid transport and delivery into cells operates mainly via two receptor-mediated pathways: on the one hand via the LDL receptor and on the other hand via the LDL receptor-related protein (LRP) receptor, which was recently discovered.<sup>[22]</sup> Lipoprotein binding to the receptors induced by interactions with ApoE initiates an endocytotic cellular uptake of the ligand–receptor complex and degradation of the lipoproteins within the cells.<sup>[28]</sup> Lipoprotein metabolism is influenced by the primary, secondary, and supramolecular apolipoprotein conformation in solution.<sup>[29]</sup> ApoE is composed of 299 amino acids possessing a molecular mass of  $\approx 34$  kDa.<sup>[30]</sup> The secondary structure of ApoE possesses two separate structural domains: the amino terminal two-thirds of the molecule and the carboxy-terminal one-third of the molecule, connected by a hinge region (Figure 3). The amino-terminal domain, composed of a four-helix bundle, contains lysine and arginine rich receptor-binding sites, whereas the carboxyl-terminal domain includes the major lipid-binding site located in amphipathic alpha-helices. The three major isoforms

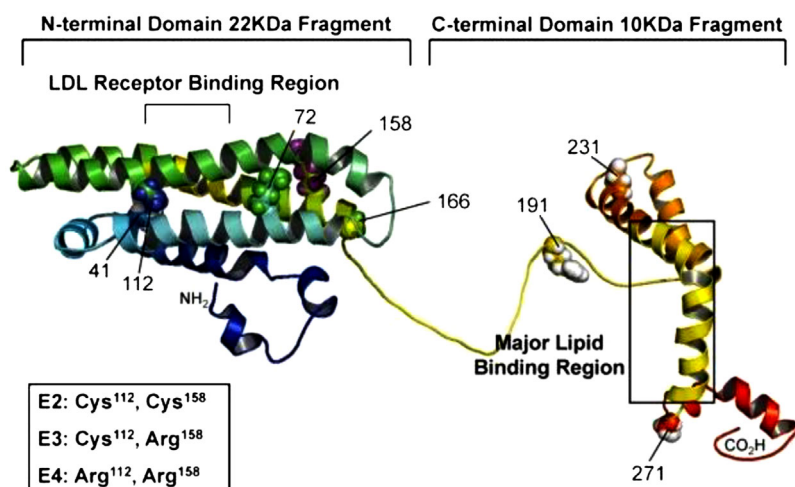


**Figure 3.** Structure of ApoE. Reproduced according to the terms of the CC-BY license.<sup>[118]</sup> Copyright, 2011, The authors.

(ApoE2, -E3 and -E4) differ only in single amino acid substitutions at two positions, which profoundly affect their structures and explain their different ability to bind lipids and receptors.<sup>[31]</sup>

### 3.2. LDL and LRP Receptors

The groups of LDL and LRP receptors belong both to the LDL receptor family, a group of cell surface receptors that transport several macromolecules into cells. In humans, the LDL receptor family includes in addition the very low-density lipoprotein (VLDL), the ApoER2 and the sorLA/LRP11 receptors. Each member is expressed in several different tissues, has a wide range of suitable ligands and is involved in various physiological functions.<sup>[11]</sup> LDL receptors are mainly expressed by liver and adrenal tissues, but can, among others, also be found in the brain, lung, heart, and kidney. LRP receptors are highly expressed in liver, brain, and lung tissues.<sup>[11a]</sup> The LDL and LRP receptors play a crucial role in the homeostasis of triglycerides and cholesterol by mediating cellular uptake of ApoE (and also ApoB in case of LDL receptor)-containing lipoprotein particles. The receptors consist of several distinct domains with individual function. The LDL receptor ligand binding domain, a cluster of seven complement-like cysteine-rich repeating units can be found on the extracellular side. This domain is followed by a sequence with similarities to the membrane-bound precursor of the epidermal growth factor (EGF), which is important for ligand uncoupling in acidified endosomes.<sup>[12]</sup> The receptor is anchored in the plasma membrane by a third important functional region, followed by several cytoplasmatic domains for endocytosis and interaction motifs for a variety of cytoplasmatic adaptor and scaffolding proteins. The LRP receptor is more complex and larger than the LDL receptor.<sup>[32]</sup> In contrast to the LDL receptor, which specifically interacts with ApoE and ApoB ligands, the LRP receptor is a multifunctional multiligand receptor and is therefore able to bind several ligands, such as ApoE, plasminogen activators, and protease/inhibitor complexes.<sup>[11a]</sup> So far, controversial information has been reported regarding the func-

tion of the LRP receptor in literature. In several studies, LRP1 is described as the main brain clearance receptor, especially in the case of amyloid  $\beta$  ( $A\beta$ ) peptides.<sup>[11b,c]</sup> However, other studies indicate that LRP1 is more likely expressed in pericytes than in endothelial cells and may not be involved in the efflux of  $A\beta$  peptides on the endothelial level.<sup>[11d]</sup> This discrepancy could be related to the different cell models used and points out that the function of the receptor is not yet fully clarified. As lipoprotein transport across the BBB is of crucial importance for the delivery of essential lipids to the brain, endothelial cells of the BBB are equipped with LDL and LRP receptors.<sup>[33]</sup> An ApoE-based transport system which is recognized by LDL receptors offers the possibility to traffic substances across the BBB and therefore provides a highly promising pathway for drug delivery into the brain.

## 4. Approaches for ApoE-Functionalization of Polymeric Nanoparticles

Organ distribution of drug-loaded NPs, in this regard also for reaching the brain, is regulated by the immediate adsorption of plasma proteins onto these particles after intravenous injection.<sup>[34]</sup> These protein adsorption patterns on the surface can depend on the physicochemical characteristics of the particles.<sup>[35]</sup> Thereafter, amount of proteins as well as adsorption of specific proteins influence macrophage uptake and in turn the organ distribution.<sup>[34]</sup> In addition, uptake into different organs can be shifted by attachment of receptor-specific ligands to the particles.

### 4.1. Surfactant-Based Approach

#### 4.1.1. Initial Protein Adsorption Experiments Using Model Carrier

First attempts on organ biodistributions with surfactant-coated polymers were performed by Illum and Davis using poly(styrene)

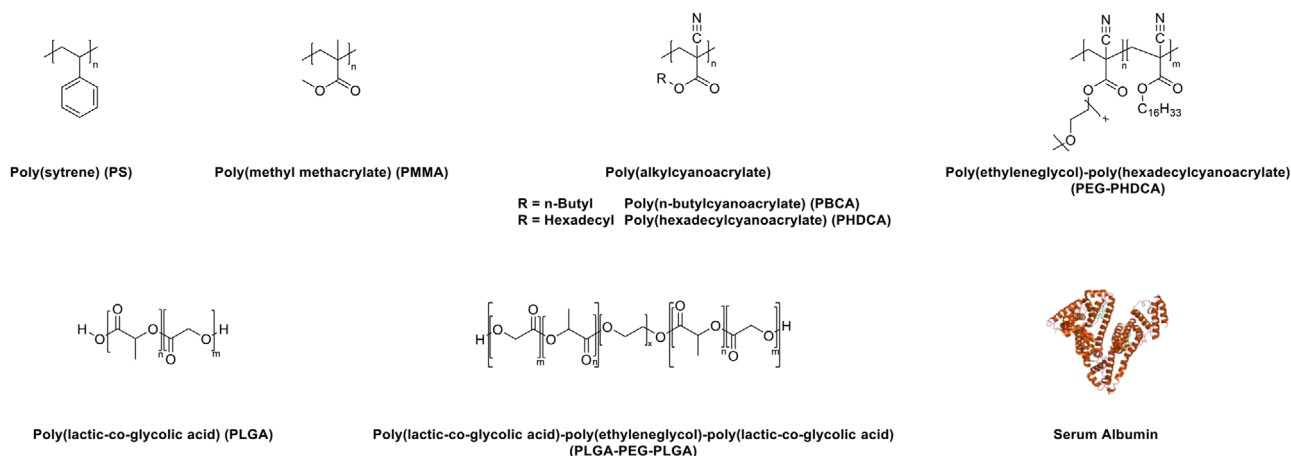


**Figure 4.** Commonly used (bio)polymers for investigation of ApoE-mediated brain targeting.

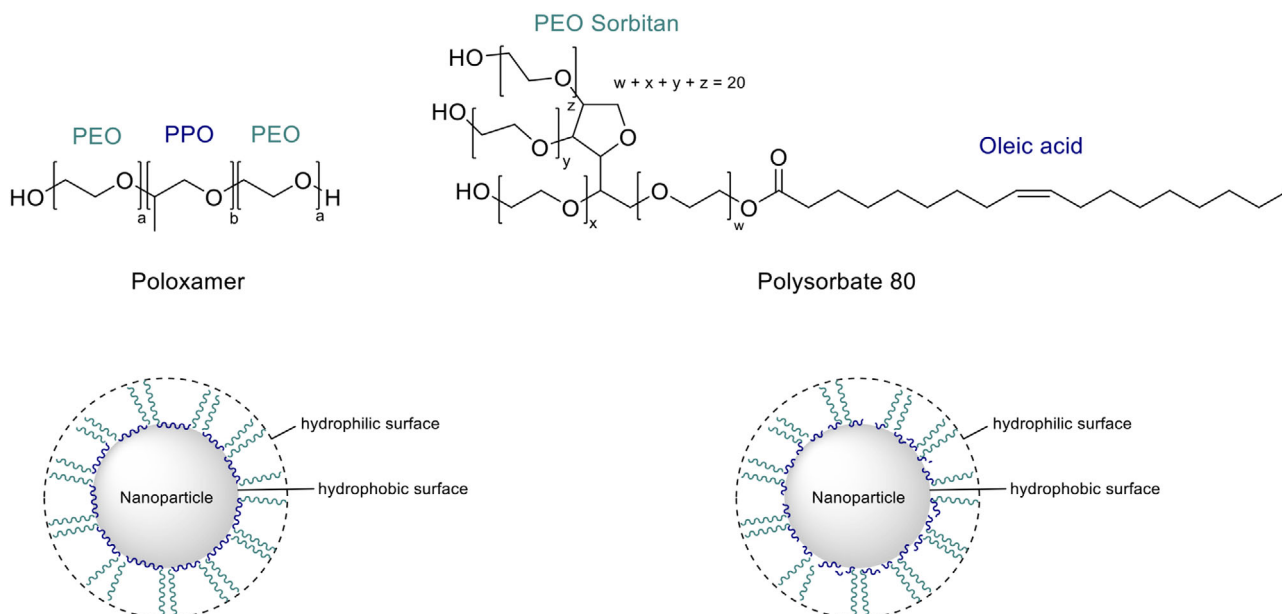


**Figure 5.** Poloxamer- and polysorbate-coating of hydrophobic nanoparticles.<sup>[34]</sup>

(PS) as a model carrier (**Figure 4**). PS is a hydrophobic, but not biodegradable polymer, which was coated with poloxamer or poloxamine followed by intravenous injection. As a consequence of coating, nanoparticle uptake was shifted from reticuloendothelial system (RES)-organs (liver and spleen) to other tissues.<sup>[36]</sup>

The specific adsorption pattern of proteins was tested in 1993 by Müller et al. with well-defined hydrophobic polystyrene beads using poloxamers.<sup>[34]</sup> Poloxamers adsorb with their hydrophobic part (poly(propylene oxide) (PPO)) at the nanoparticle, whereas the hydrophilic part (poly(ethylene oxide) (PEO or PEG) protrudes into the dispersion medium, exposing a hydrophilic surface, which can be modified when using poloxamers with different polarity by varying hydrophobic/hydrophilic ratio (**Figure 5**).

These differently constituted poloxamers facilitate the adsorption of specific proteins. To determine amounts of adsorbed proteins (e.g., albumin, fibrinogen, and apolipoproteins), the

patterns of protein adsorption onto coated beads were analyzed after incubation with plasma by high-resolution 2D polyacrylamide gel electrophoresis (2-D PAGE). Increased amounts of proteins on the surface in comparison to the amount of these proteins in the plasma were found for, e.g., transferrin or ApoC-III, which are proteins facilitating receptor-mediated uptake of nanoparticles. In general, the amount of an adsorbed protein is related to surface hydrophobicity. Overproportional fractions were found for ApoE on particles with the lowest hydrophilicity (**Figure 6A**). In contrary, quantitative differences for single proteins could not solely be correlated to the differences in surface hydrophobicity. Therefore, only measuring surface hydrophobicity is not sufficient for statements about protein adsorption patterns.<sup>[34]</sup> The same group further intensified their studies on adsorption of plasma proteins on various surfaces by synthesizing polymers in a very complex and multifaceted

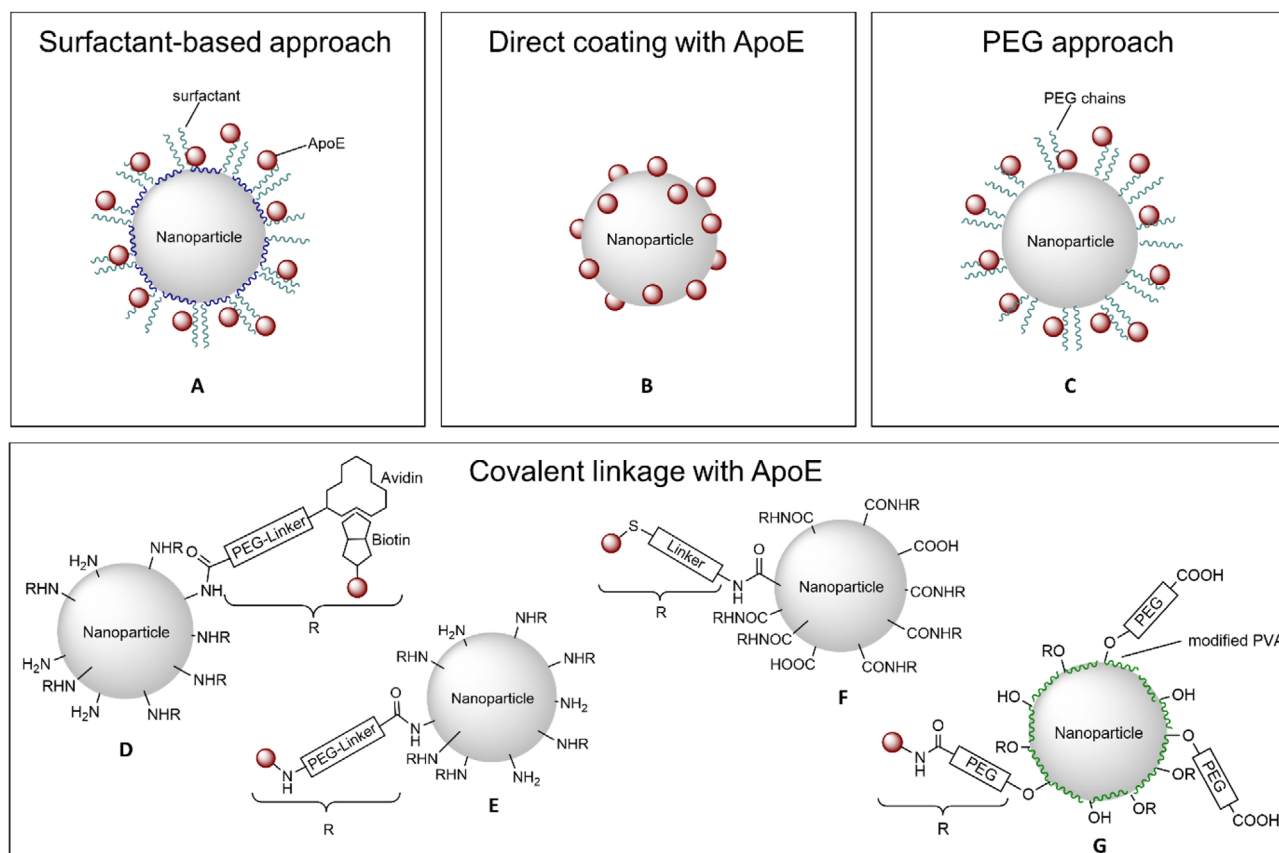


**Figure 6.** Approaches for ApoE-functionalization of polymeric nanoparticles.

approach. Five different latex type particles using styrene and different functionalized (meth)acrylates with different hydrophobicities, surface properties and surface charges were obtained. Protein adsorption onto these colloidal surfaces depended on surface properties such as hydrophobicity, charge density, and accessibility due to sterical hindrance of the surface groups. Apolipoproteins were adsorbed in slightly higher amounts on type 4 latex particles which bear different functional groups (OH, NR<sub>3</sub>) located at the end of flexible polyethylene glycol (PEG) chains. The PEG chains seem to protect the surface of the particles against adsorption of larger proteins. Hence, small proteins, such as apolipoproteins, despite having a lower affinity to the surface, probably could adsorb to binding sites of particle type 4, when they are not occupied by larger proteins. Nevertheless, the impact of apolipoproteins on the total adsorbed protein amount was very low compared to that of the larger proteins.<sup>[35]</sup>

First attempts in determining *in vivo* organ distribution were realized with coated and uncoated radiolabeled poly(methyl methacrylate) (PMMA) particles (Figure 4). <sup>14</sup>C-labeled nanoparticles were prepared by radiation-induced polymerization of methyl[2-<sup>14</sup>C]methacrylate.<sup>[38]</sup> Coating was performed with nonionic surfactants such as poloxamers/poloxamines, polysorbates or polyoxyethylene lauryl ether.<sup>[37]</sup> A prolonged circulation time in the blood stream was induced by steric repulsion of these surfactant-coated PMMA NPs and led to reduction of adsorption onto surfaces of macrophages. Thus, a lower particle

concentration in RES organs and tissues such as liver, spleen, bone marrow and lymph nodes was observed. Significantly higher levels in the blood and non-RES organs (heart, gastrointestinal tract, ovary, kidneys, muscles, and brain) were obtained after coating with either surfactants. Poloxamer and poloxamine (i.e., poloxamer 338 and poloxamine 908) were the most efficient ones in decreasing liver uptake, while increasing the blood levels of NPs by a factor of 100 or higher. In the brain, the uptake of nanoparticles was increased for all surfactants up to 13-fold, especially nanoparticle coatings with polysorbate 80 and 60 and different poloxamers, except poloxamer 188, were the most efficient.<sup>[37]</sup>

These surfactant-coated radiolabeled PMMA NPs were also tested in an uptake study using bovine microvessel endothelial cell (BMEC) monocultures. Coating with polysorbate 80, the most efficient surfactant for *in vivo* brain targeting, showed also a promising performance in *in vitro* nanoparticle uptake, which was enhanced by a factor of 5 compared to the control group (uncoated PMMA NPs). However, distinction between uptake and cell attachment could not be made using their experimental setup.<sup>[39]</sup>

#### 4.1.2. Poly(alkylcyanoacrylates)

Not only the surfactant, but also the type of solid particle, i.e., the hydrophilicity of the particle, has an influence on the

body distribution. Because PMMA and PS are quite similar regarding their hydrophobicity, similar affinity to surfactants was expected.<sup>[40]</sup> Poly(alkylcyanoarylates), especially PBCA (Figure 4), show a much higher hydrophilicity. In addition, a very rapid degradation via ester hydrolysis was confirmed, so that drug release for these polymers occurs due to degradation.<sup>[41]</sup> In addition, *in vivo* and *in vitro* studies demonstrated that PBCA is nontoxic, but until now poly(alkylcyanoacrylates) are not approved for intravenous administration by the US Food and Drug Administration (FDA).<sup>[42]</sup>

First attempts to use PBCA NPs for transport of drugs across the BBB were performed with the hexapeptide dalargin. The analgesic effects of this drug were studied simultaneously by two independent groups using different pain assessment methods (tail flick test<sup>[43]</sup> vs hot-plate test<sup>[44]</sup>). Both drug delivery systems consisted of PBCA, dalargin and polysorbate 80. Nanoparticles were prepared using *n*-butyl cyanoacrylate and dextran 70 000 as stabilizer in an acidic polymerization medium. The peptide dalargin was then adsorbed onto the nanoparticle surface and afterwards polysorbate 80 was added. These studies demonstrated that binding of dalargin to the PBCA NPs as well as coating of these NPs with polysorbate 80 are mandatory to promote dalargin uptake into the brain.<sup>[43–45]</sup> In a further in-depth study, 12 different surfactants for coating onto dalargin-containing PBCA NPs were tested. Solely coating with polysorbate 20, 40, 60, and 80 had a significant effect on the successful passage of dalargin across the BBB *in vivo*, in which polysorbate 80 was the most efficient one. In addition, NPs with polysorbate 80 coating, but without dalargin had no effect. The authors suggested a specific alteration of the PBCA surface properties due to coating with polysorbates. In accordance with previous studies, adsorption of only specific substances from the blood which induce endocytosis from the blood by the endothelial cells of the BBB was assumed.<sup>[46]</sup>

Body distribution of <sup>3</sup>H-dalargin-loaded, polysorbate 80-coated PBCA was analyzed after intravenous injection into mice. Radioactivity levels, caused by <sup>3</sup>H-dalargin, were three-times higher in the brain and reduced in the liver when the drug-loaded and polysorbate-coated PBCA NPs were used.<sup>[45,47]</sup>

The influence of polysorbate 80-coated and uncoated PBCA NPs on the BBB integrity of porcine brain capillary endothelial cells (PBCEC) cultured on microporous Transwell filter inserts was studied via transendothelial electrical resistance (TEER) measurements. The integrity of the BBB was also analyzed by measuring the passage of <sup>14</sup>C-sucrose and FITC-BSA (fluorescein isothiocyanate labeled bovine serum albumin) as reference substances. The application of polysorbate 80-coated PBCA NP led to a reversible disruption of the barrier. After 24 h the TEER of cells treated with 13  $\mu\text{g mL}^{-1}$  NP recovered to about 80% of the starting value. Further lowering the NPs concentration led to a nearly complete recovery of the barrier integrity. The obtained increased permeability of <sup>14</sup>C-sucrose and FITC-BSA about 4 h after nanoparticle application were conflicting with other measurements regarding the permeability of the BBB after treatment with polysorbate 80-coated PBCA.<sup>[48]</sup> Another criticism that brain delivery with polysorbate 80-coated PBCA NPs occurs due to toxic effects of the carrier arose after using an *in vitro* BBB model of a coculture of bovine brain capillary endothelial cells (BBCEC) and rat astrocytes. The observed toxicity led to

opening of the tight junctions allowing the penetration of drugs through the BBB and thus leading to therapeutic limitations of PBCA NPs when NPs with concentrations of 10  $\mu\text{g mL}^{-1}$  and above were used.<sup>[49]</sup> As a consequence of these statements, prior binding of dalargin to the nanoparticles is not mandatory and the drug can also diffuse into the brain after carrier-induced opening of the tight junctions when polymer and drug are injected shortly after each other. This assumption was rejected by Begley and co-workers in 2002 using *in vivo* and *in vitro* human, bovine, and rat models. In order to evaluate this hypothesis *in vivo*, free dalargin was injected intravenously into mice after the injection of polysorbate 80-coated, but empty NPs. Analgesic effects were only obtained when the drug was adsorbed onto the NPs and the thesis of diffusional dalargin entry was not supported. *In vitro*, the permeability of <sup>14</sup>C-sucrose and <sup>3</sup>H-inulin, as model substances, was not changed after PBCA preincubation at concentrations of 10 or 20  $\mu\text{g mL}^{-1}$ . Incubation of uncoated and polysorbate-80-coated PBCA NPs showed a normal morphology of the endothelial cells, again emphasizing a lack of toxicity. The bovine endothelial cells appeared intact without any evidence of available paracellular pathways. However, the authors observed undefined changes at the cell membranes by electron microscopy when using polysorbate-80-coated PBCA NPs.<sup>[50]</sup>

Cultured microvessel brain endothelial cells of human and bovine origin were used, to gain deeper insights into the uptake mechanism of polysorbate 80-coated PBCA NPs. These cells express high levels of LDL receptor, which seems to play an important role in the uptake of polysorbate 80-coated NPs, due to adsorption of apolipoproteins onto the NPs' surface. Indeed, the uptake of polysorbate-coated PBCA NPs in these cells was 20-times higher compared to uncoated counterparts. Inhibition experiments revealed that nanoparticles were taken up via an endocytic mechanism. Phagocytosis, which is caused by apolipoprotein components, provoked uptake. This was concluded because uptake was inhibited by cytochalasin, a phagocytic uptake inhibitor. Pinocytosis was not observed, since uptake was not inhibited by colchicine, a pinocytic uptake inhibitor.<sup>[13]</sup>

Besides intravenous injection, oral delivery of dalargin-loaded PBCA NPs coated with polysorbate 80 was tested as another administration route. For comparison reasons, dalargin-bound PBCA NPs were applied intravenously and orally and *in vivo* dalargin-induced analgesia was used to amount the efficiency of BBB passage by hot-plate test. PBCA NPs were prepared in acidic medium using polysorbate 85, dextran 12 000 or poloxamer 188 as stabilizers. Similar to the before mentioned methods, dalargin was subsequently attached to the nanoparticles before coating with polysorbate 80 was performed. Polysorbate 85-stabilized, dalargin-loaded, but uncoated PBCA NPs were able to induce analgesic effects in mice after intravenous and oral application even when NPs were not coated. Dextran 12 000 or poloxamer 188-stabilized, dalargin-loaded, uncoated NPs showed no significant effect after oral administration.<sup>[51]</sup> Oral administration was also tested with double-coated dalargin-loaded PBCA NPs. Tail-flick tests showed that dalargin-induced analgesia was higher with PBCA NPs prepared with double coating of polysorbate and PEG compared to single coating. As a result, surfactant-coated PBCA NPs are able to cross the gastrointestinal barrier after oral administration. Nevertheless, the exact mechanisms of

**Table 1.** Peptides/proteins encapsulated in polymeric nanoparticles for ApoE-mediated brain targeting.

Drug <sup>a)</sup>	Disease/effect of drug	Nanoparticulate formulation	Type of ApoE-functionalization	In vivo data	[Refs.]
Dalargin (Hexapeptide)	Analgesia	PBCA	Indirect by PS80 coating	Yes	[43–45,51,74,110,119]
		PBCA	Indirect by different PS coatings	Yes	[46,119a]
		PBCA	Indirect by PEG 20 000 and/or PS80 coating	Yes	[52]
		PBCA	Coating with ApoE (and PS80)	Yes	[59,60]
Kyotorphin (Dipeptide)	Analgesia	PBCA	Indirect by PS80 coating	Yes	[74]
Morphiceptin (Tetrapeptide)	Analgesia	PBCA	Indirect by PS80 coating	Yes	[120]
Endomorphin-1 (Tetrapeptide)	Analgesia	PBCA	Indirect by PS80 coating	Yes	[121]
Nerve growth factor	Alzheimer's disease	PBCA	Indirect by PS80 coating	Yes	[75,76]
	Parkinson's disease				
	Stroke	Iron oxide and HSA	Covalent linkage of ApoE	Yes	[77]
BDNF	Traumatic brain injury	PLGA	Indirect by poloxamer 188-coating	Yes	[78]
Arylsulfatase A	Metachromatic leukodystrophy	PBCA	Indirect by PS80 coating	No	[122]
		PLA	Indirect by poloxamer 188-coating	No	[122]
		PLGA	Indirect by poloxamer 188-coating	No	[122]
		HSA	Indirect by PS80 coating	No	[122]

<sup>a)</sup> PS80, polysorbate 80.

nanoparticulate uptake through the gastrointestinal barrier was not elucidated.<sup>[52]</sup>

#### 4.1.3. Poly(lactic-co-glycolic acid)

Poly(lactic-co-glycolic acid) (PLGA) is considered for brain targeting across the BBB due to FDA approval of other drug formulations containing PLGA for human use combined with conducive biocompatibility and biodegradability profiles (Figure 4).<sup>[53]</sup> The first study on surfactant-coated, drug-loaded PLGA NPs for brain delivery after intravenous injection was performed by Kreuter et al. in 2010 with poloxamer 188 and polysorbate 80 as surfactants. The PLGA NPs were prepared by a multistep emulsification–solvent evaporation technique with different modifications depending on which drug was used (i.e., doxorubicin or loperamide). For PLGA, the most efficient brain delivery was achieved by binding of these drugs to poly(vinyl alcohol) (PVA)-stabilized NPs coated with poloxamer 188. The antitumor effect of doxorubicin was evaluated in a rat model of glioblastoma. To compare PLGA to PBCA NPs, experiments were planned similarly to PBCA experiments regarding surfactants, drugs, and animal models. For both polymers, uncoated NPs were ineffective. Coating with polysorbate 80 led to highest efficiencies for PBCA NPs, whereas poloxamer 188-coating performed best for PLGA NPs.<sup>[54]</sup>

The mechanism by which doxorubicin-loaded poloxamer 188-coated PLGA NPs enter brain tumor cells was elucidated by uptake experiments in human glioblastoma cells without investigating the passage of the BBB. The main mechanism of the NP internalization was clathrin-mediated endocytosis. It was demonstrated that the main mechanism of release of the drug was due to doxorubicin diffusion from the NPs rather than by intracellular degradation of the polymer, because free

doxorubicin reached the nuclei, whereas PLGA was still present in the endosomes/lysosomes.<sup>[85]</sup>

A similar drug delivery system was developed by Lee et al. who used poly(lactide-co-glycolide)–poly(ethylene glycol)–poly(lactide-co-glycolide) (PLGA–PEG–PLGA) triblock copolymers (Figure 4). This polymer was synthesized by ring-opening polymerization using PEG as a macroinitiator. Loperamide-loaded PLGA–PEG–PLGA (PEP) NPs were prepared by a nanoprecipitation method and then the NPs were coated with poloxamer 188 or polysorbate 80. For an in vitro BBB penetration study, a culture of immortalized rat brain endothelial cell line and C6 glioma cells was established. It was shown that surfactant-coated PEP NPs had a better penetration than uncoated PEP NPs and poloxamer 188-coated PEP NPs showed higher cellular uptake than polysorbate 80-coated ones. However, the group did not include TEER measurements during their study to validate the intact coculture setup.<sup>[55]</sup>

#### 4.1.4. Other Materials

In addition to the before mentioned polymers, individual investigations were also performed with other polymeric NPs (Tables 1 and 2).

Polycaprolactone (PCL) NPs loaded with the small drug pentamidine were compared to liposomes regarding in vitro transport across the BBB with the aim of treating Human African Trypanosomiasis. These pentamidine-loaded PCL NPs were obtained by double solvent evaporation method. Polysorbate 80 was used as a surfactant to obtain ApoE adsorption facilitating transport across the BBB. The study revealed that liposome nanocarriers were able to transport a larger dose percentage of pentamidine compared to PCL NPs and that drug loading in PCL NPs needed optimization.<sup>[56]</sup> Based on these observations, PCL NPs



**Table 2.** Small molecules encapsulated in polymeric nanoparticles for ApoE-mediated brain targeting.

Drug	Disease/effect of drug	Nanoparticulate formulation	Type of ApoE-functionalization	In vivo data	[Refs.]
Loperamide	Analgesia	PBCA	Indirect by PS80-coating	Yes	[79b]
		PBCA	Coating with ApoE	Yes	[59]
		HSA	Covalent linkage of ApoE	Yes	[68,71]
		PLGA	Indirect by PS80- or poloxamer 188-coating	Yes	[54]
		PLGA-PEG-PLGA	Indirect by PS80- or poloxamer 188-coating	Yes	[55]
Doxorubicin	Cerebral cancer	PBCA	Indirect by PS80-coating	Yes	[79c,80,82]
		PLGA	Indirect by PS80- or poloxamer 188-coating	Yes	[54,85]
		PDMA-PS	Coating with mApoE	No	[86a]
Doxorubicin	Brain metastases	PMA-PS80-starch	Indirect by PS80	Yes	[86b]
Methotrexate	Cerebral cancer	PBCA	Indirect by PS80-coating	Yes	[87]
Temozolomide	Cerebral cancer	PBCA	Indirect by PS80-coating	Yes	[88]
Cisplatin	Cerebral cancer	PBCA	Indirect by PS80-coating	Yes	[89]
Carboplatin	Cerebral cancer	PLGA	Indirect by PS80-coating	Yes	[123]
Docetaxel	Brain metastases	PMA-PS80-maltodextrin-dodecane	Indirect by PS80	Yes	[124]
Docetaxel	Cerebral cancer	PLGA-PEG-DHA	Indirect by PEG and DHA	Yes	[125]
Gemcitabine	Cerebral cancer	PBCA	Indirect by PS80-coating	Yes	[126]
Curcumin	Cerebral cancer	PBCA	Coating with ApoE	No	[90a]
Curcumin	Alzheimer's disease	PBCA	Coating with ApoE	No	[90b]
Tacrine	Alzheimer's disease	PBCA	Indirect by PS80-coating	Yes	[91a,127]
		PBCA-PEG	Indirect by PEG	Yes	[127]
Rivastigmine	Alzheimer's disease	PBCA	Indirect by PS80-coating	Yes	[91b]
Estradiol	Alzheimer's disease	PLGA	Indirect by PS80-coating	Yes	[92]
Rosmarinic acid	Alzheimer's disease	PAAM-CH-PLGA	Coating with ApoE	Yes	[61]
Salvianolic acid B	Neurodegenerative diseases	PECA	Indirect by PS80-coating	Yes	[128]
Tubocurarine	Muscle relaxation	PBCA	Indirect by PS80-coating	Yes	[79a]
Pentamidine	Human African trypanosomiasis	PCL	Indirect by PS80-coating	No	[56]
Amitriptyline	Depression	PBCA	Indirect by PS80-coating	Yes	[74]
MRZ 2/576	Epilepsy	PBCA	Indirect by PS80-coating	Yes	[129]
Valproic acid	Epilepsy	PBCA	Indirect by PS80-coating	Yes	[130]
Breviscapine	Cerebrovascular diseases	PLA	Indirect by poloxamer 188-coating	Yes	[131]
Puerarin	Stroke	PBCA	Indirect by PS80-coating	Yes	[132]
Gatifloxacin	Central nervous system tuberculosis	PLGA	Indirect by PS80-coating	Yes	[133]
Amphotericin B	Cryptococcal meningitis	PBCA	Indirect by PS80-coating	Yes	[134]
		PLA-PEG	Indirect by PS80-coating and PEG	Yes	[135]
Quercetin	Antioxidant	PBCA	Indirect by PS80-coating	Yes	[136]
Stavudine	Human immunodeficiency virus	PBCA	Indirect by PS80-coating	No	[137]
Delavirdine	Human immunodeficiency virus	PBCA	Indirect by PS80-coating	No	[137]
Saquinavir	Human immunodeficiency virus	PBCA	Indirect by PS80-coating	No	[137]
Obidoxime	Acetylcholinesterase reactivator	HSA	Covalent linkage of ApoE	No	[138]
Sumatriptan succinate	Migraine	PBCA	Indirect by PS80-coating	Yes	[139]
		BSA	Covalent linkage of ApoE	Yes	[139]

<sup>a)</sup> PS80, polysorbate 80; PDMA, poly(dimethylacrylamide); PMA, poly(methacrylic acid); PECA, poly(ethylcyanoacrylate), BSA, bovine serum albumin.

seem not to exhibit the desired carrier properties for drug delivery across the BBB.

Superparamagnetic iron oxide nanoparticles (SPIONs) decorated with PEG, poly(ethylenimine) and polysorbate 80 resulting in Tween-SPIONs were prepared for brain targeting. Intravenously administrated Tween-SPIONs actively crossed the BBB of rats under an external magnetic field (EMF), and a significant

amount of SPIONs was found in the cortex. Both the surfactant and the magnetic field played a crucial role in transportation of SPIONs across the BBB. It was suggested that the positively charged Tween-SPIONs adsorb apolipoproteins in the blood. With the assistance of EMF, the contact with the endothelial cells is improved promoting receptor-mediated endocytosis.<sup>[57]</sup> A similar approach was conducted with magnetic nanoparticles

(MNPs) made from PS nanospheres. These Fe<sub>3</sub>O<sub>4</sub>/PS nanospheres were suspended in a polysorbate aqueous solution and can cross the intact BBB after intravenous injection when subjected to an EMF. The role of the surfactant was not discussed in this manuscript. In addition, a large fraction of the magnetic NPs was cleared from the circulation by liver and spleen.<sup>[58]</sup>

#### 4.2. Direct Coating with ApoE

To further investigate the involvement of apolipoproteins in the transport of drug-loaded NPs across the BBB, dalargin- and loperamide-loaded PBCA NPs were directly coated with apolipoproteins AII, B, CII, J, and E with and without additional precoating with polysorbate 80 (Figure 6B). Afterwards, these different nanoparticulate formulations were intravenously injected into mice and their efficiency was calculated by tail-flick test, since both drugs induce an analgesic effect. It was shown that solely drug-bound NPs coated with polysorbate 80 and/or with ApoB or ApoE induced the desired effects.<sup>[59]</sup> In general, these effects were higher in case of ApoE-functionalization than with ApoB, making ApoE an ideal candidate for brain targeting across the BBB. The most pronounced effect was observed after precoating with polysorbate 80 and additional coating with apolipoproteins, caused by additional adsorption of apolipoproteins from blood plasma after intravenous injection.<sup>[59,60]</sup> These findings were substantiated by *in vivo* experiments with genetically modified ApoE-deficient mice in which drug-containing NPs showed lower effects compared to experiments using non-modified mice. These experiments confirmed the suggestion that apolipoproteins are involved in the uptake mechanism of polysorbate 80-coated NPs by adsorption of these proteins from the blood after intravenous injection. ApoE-functionalized NPs mimic lipoproteins that are able to enter the brain capillary endothelial cells via LDL receptor-mediated endocytosis. Drugs are then further transported by diffusion or by transcytosis. The authors also mentioned in this context that apolipoproteins only facilitate the interaction with the endothelial cells, but are not taken up together with the NPs.<sup>[59]</sup>

One approach to directly coat NPs with ApoE was carried out by Kuo et al. using rosmarinic acid-loaded poly(acrylamide)-chitosan-poly(lactide-co-glycolide) (RA-PAAM-CH-PLGA) NPs anchoring two targeting biomolecules. Rosmarinic acid, an antioxidant with anti-allergenic and anti-inflammatory activity was encapsulated for the potential treatment of Alzheimer's disease. Cross-reacting material 197 (CRM197), a ligand of the diphtheria toxin receptor, and ApoE, which can recognize LDL receptors, were expected to facilitate transcytosis across brain-microvascular endothelial cells. PLGA was used as the hydrophobic core and hydrophilic PAAM and chitosan entrapped the drug. The polymeric nanocarriers were prepared by a complex method consisting of microemulsion, solvent diffusion, grafting, and surface modification to obtain CRM197-ApoE-RA-PAAM-CH-PLGA NPs. For uptake experiments RAW264.7 cells and for viability and permeability measurements SK-N-MC cells and cocultures of human BMECs (HBMECs) and astrocytes were used. The results revealed that a higher PAAM-percentage decreased the grafting efficiency of CRM197 and ApoE. Additionally, an increase in CRM197 and ApoE enhanced the ability

of rosmarinic acid to cross the BBB and inhibited apoptosis of A $\beta$ -insulted SK-N-MC cells to a larger extent.<sup>[61]</sup>

#### 4.3. PEG Approach

An advanced system was developed by Couvreur et al. who incorporated PEG-chains to poly(alkylcyanoacrylates) to induce an *in vivo* long-circulating ("stealth") effect and investigated the biodistribution of such systems after intravenous administration to mice. PEG-cyanoacrylate copolymers were prepared by condensation of methoxy-poly(ethylene glycol)cyanoacrylate and [3-<sup>14</sup>C]-n-hexadecyl-cyanoacrylate in different ratios (Figure 4). It was observed that these [<sup>14</sup>C]-radiolabeled PEGylated poly(hexadecylcyanoacrylate) (PEG-PHDCA) NPs remained longer in the blood circulation and had a reduced cytotoxicity compared to non-PEGylated PHDCA NPs which were cleared in a few minutes.<sup>[62]</sup> Further increasing the PEG-amount in the PEG-PHDCA copolymers had no effect on *in vivo* blood circulation time in this study, but had a positive effect regarding toxicity in *in vitro* studies on PEG-coated poly(alkylcyanoacrylates).<sup>[62,63]</sup> Liver accumulation was drastically reduced, however an increased spleen uptake was shown.<sup>[62]</sup> Accumulation in the brain was first tested with these systems in 2001 by the same group by investigating biodistribution profiles, brain concentrations and brain distributions of radiolabeled PEG-PHDCA in comparison to polysorbate 80- or poloxamine 908-coated PHDCA NPs *in vivo* in rats and mice. Based on the before observed long-circulating characteristics of PEGylated PHDCA NPs, these NPs enter the brain to a larger extent than NPs without PEGylation or with surfactant-coating. In addition, the stealth effect was more pronounced in mice than in rats. BBB permeability was not influenced after injection of PEG-PHDCA as measured *in vivo* by diffusion of <sup>14</sup>C-sucrose into the brain.<sup>[64]</sup> Detailed analytical investigation on adsorbed proteins on the surface of PEG-PHDCA NPs after incubation with serum revealed that ApoE and ApoB adsorbed more onto PEGylated PHDCA than on unmodified PHDCA NPs (Figure 6C). As a consequence, ApoE or ApoB-100 preadsorbed onto PEG-PHDCA NPs were more efficient than unmodified PEG-PHDCA in penetrating into rat brain endothelial cells, suggesting the involvement of LDL receptor-mediated endocytosis also for PEGylated PHDCA. In addition, cellular uptake was also increased with increasing the concentrations of ApoE in ApoE-preincubated NPs.<sup>[65]</sup>

Inhibition of the cellular uptake of fluorescent-labeled PEG-PHDCA NPs with chlorpromazine and sodium azide, which inhibit clathrin and energy-dependent endocytosis, respectively, caused a significant decrease in uptake. Inhibition of the caveolae-mediated pathway by preincubation with filipin and nystatin did not alter the cellular uptake. The confirmation of involvement of LDL receptor was confirmed by blocking ligand-binding LDL receptors using anti-LDLR mAb which caused a drastic decrease in uptake of ApoE-precoated PEG-PHDCA.<sup>[66]</sup>

However, in preclinical tests, doxorubicin-loaded PEG-PHDCA failed to induce a therapeutic effect in 9L gliosarcoma models and accumulation was about three times lower in the tumor in comparison to unloaded PEG-PHDCA NPs. Aggregation with plasma proteins due to higher positive charge of the doxorubicin-loaded PEG-PHDCA NPs is suggested which

might hinder efficient therapeutic effects which is not observed using surfactant-coated NPs (e.g., PBCA or PLGA) in the same gliosarcoma model. As a conclusion, stealth properties alone might not be sufficient for effective brain targeting.<sup>[67]</sup>

#### 4.4. Covalent Linkage with ApoE

Taken together the findings of studies on polysorbate 80-coated PBCA NPs, adsorption of ApoE and subsequent binding of ApoE to the LDL receptor facilitate endocytosis and/or transcytosis, which can be applied for drug transport to the brain.<sup>[59]</sup>

Another delivery system are albumin-NPs prepared from human serum albumin (HSA), which are biodegradable, easy to prepare and bear reactive groups on their surfaces, e.g., amino and carboxylic acid groups (Figure 4). These groups facilitate direct covalent ligand binding/surface modification, which can be advantageous to surfactant-coating due to concerns and contradictions regarding surfactant's toxicity.<sup>[68]</sup>

In 2006, ApoE was coupled by chemical methods covalently to HSA NPs by the group of Langer to investigate the transport of loperamide to the brain. These NPs were prepared by a desolvation method and afterwards these NPs were activated using a sulfhydryl-modified PEG cross-linker (NHS-PEG-Mal). NeutrAvidin was conjugated to the activated HSA-NP by reaction of avidin with the amino group of the bifunctional spacer. ApoE was biotinylated to enable the attachment of ApoE to NeutrAvidin-modified NPs (Figure 6D). This modification was chosen since avidin and biotin form the most stable naturally occurring complex. Investigation of these ApoE-coupled and loperamide-coated HSA NPs revealed strong antinociceptive effects, whereas nonmodified HSA-NP were unable to transport the drug across the BBB. These effects were even more pronounced than with polysorbate-coated HSA-NPs.<sup>[68]</sup> When using HSA NPs, loperamide is only adsorbed to the surface of the NPs, but all experiments revealed a stable drug attachment even in the presence of various concentrations of serum or surfactants.<sup>[68]</sup>

HSA NPs with covalently bound ApoE are taken up into brain endothelial cells by endocytosis after intravenous injection tested in vivo and in vitro with mouse endothelial (b.End3) cells. In addition, transcytosis took place as well because some of these particles were found in the brain parenchyma.<sup>[69]</sup> Studies on the exact uptake mechanism revealed the LRP1 as the receptor responsible for ApoE-HSA NPs uptake after performing in vitro experiments with bEnd3 cells using specific antibodies against the LRP1, the LDL, the ApoE-receptor and Megalin and incubation experiments.<sup>[70]</sup> A similar method for covalent binding was used to determine if a shorter linkage is possible by using thiolated apolipoproteins (reaction with Traut's reagent) and direct reaction with the heterobifunctional NHS-PEG-Mal linker without use of avidin-biotin (Figure 6E). Supplementary to ApoE, covalent attachment of ApoA-I (recognized by scavenger receptor class B type I) and ApoB-100 (recognized by LDL receptor), which interact with the brain endothelial cells partially by different mechanisms, was performed. Nevertheless, NPs with ApoE3 showed the highest antinociceptive effects.<sup>[71]</sup> In conclusion, ApoE-coupled HSA NPs are a surfactant-free and well-defined system for efficient transport of loperamide across the BBB.

One of the first approaches for direct coupling of PLGA to ApoE was performed with an ApoE-modified peptide (pep-apoE), which was previously successfully evaluated with lipid NPs.<sup>[72]</sup> A single emulsion solvent evaporation method was used for preparing the PLGA NPs. PLGA NPs were conjugated with pep-apoE using an appropriate linker for the carboxylic acid groups of PLGA and thiol-groups of the peptide (Figure 6F). After intravenous injection in mice, ApoE-functionalized, but not nonfunctionalized, fluorescent PLGA NPs were detected in the cerebral cortex parenchyma. However, a weak fluorescence signal was also detected after injection of ApoE-functionalized PLGA NPs in liver sections.<sup>[72a]</sup>

A new preparation strategy for surface modified poly(lactic acid) (PLA) NPs was established by Langer and co-workers in 2018 to enhance uptake by endothelial cells. In order to achieve an active targeting to the brain, a covalent linkage of ligands, i.e., ApoE, penetratin and ovalbumin to the nanoparticles' surface was performed by a vinyl sulfone-modified poly(vinyl alcohol)-derivative (VS-PVA), a newly developed steric stabilizer bearing reactive vinyl sulfone-groups (Figure 6G). This modified stabilizer was introduced as a facile route for ligand coupling reactions directly to PVA-stabilized NPs. The problem of inaccessibility of the polymers' carboxylic groups hindering covalent surface modification by coating with commonly used, but unreactive PVA was overcome by this approach. NPs were prepared by an emulsification-diffusion method. For preparation of protein-modified PLA NPs, the surface of the NPs was PEGylated by reaction of the vinyl-sulfone groups of VS-PVA-PLA with the amino groups of  $\alpha$ -amino- $\omega$ -carboxy PEG chains. Afterward, ApoE and ovalbumin were coupled to the PEG chains by esterification. Penetratin was coated onto the surface of the NP without using PEG spacer. Penetratin- (a cell-penetrating peptide) and ApoE-modified VS-PVA-PLA NPs showed a significantly higher cellular uptake than ovalbumin-modified or unmodified NPs as control formulations. In conclusion, an effective approach to couple ligands to PLA surfaces was established,<sup>[73]</sup> but in vivo studies were not conducted.

## 5. Drug Formulation

### 5.1. Peptides and Proteins

To investigate another neuropeptide besides dalargin (vide supra) which induces analgesia, Schröder et al. used kyotorphin, a dipeptide which normally does not cross the BBB, because of its hydrophilicity (Table 1). NPs modified with kyotorphin, dalargin, and amitriptyline, which is known to normally penetrate the BBB as a drug, were compared. After the adsorption of the peptide dalargin on polysorbate 85-stabilized PBCA NPs, analgesia was observed by hot-plate test in mice after intravenous application even when NPs were not coated with polysorbate 80. The use of Dextran 70 000 as stabilizer during acidic nanoparticle preparation in parallel experiments led to the need of polysorbate coating after attachment of the drug (dalargin or kyotorphin) to be capable of inducing analgesia. In addition, even the amitriptyline level was significantly increased in the brain with amitriptyline-loaded PBCA NPs in comparison to the free drug.<sup>[74]</sup>

Nerve growth factor (NGF), a neuropeptide, adsorbed on polysorbate-80 PBCA NPs was used to study the antiparkinsonian effect in the CNS. C57B1/6 mice were treated with 1-methyl-4-phenyl-1,2,3,6-tetrahydropyridine to provoke parkinsonian syndrome. After treatment of NGF-adsorbed polysorbate 80-coated PBCA NPs, symptoms of Parkinson's disease were decreased as shown by a lower rigidity and increased locomotor activity.<sup>[75]</sup> Brain delivery of similar NPs was also evaluated in the model of acute scopolamine-induced amnesia in rats. Using the passive avoidance reflex (PAR) test, intravenous administration of NGF polysorbate 80-coated PBCA NPs successfully reversed scopolamine-induced amnesia and enhanced recognition and memory. Direct measurement of NGF concentrations in the murine brain confirmed that polysorbate 80-coated PBCA NPs enable transit across the BBB after intravenous injection.<sup>[76]</sup>

For the treatment of stroke, therapeutic NGF and ultrasmall iron oxide particles (USPIO), for diagnostic functionality to track the *in vivo* biodistribution, were coencapsulated into a chemically crosslinked HSA matrix. Modification of the particle surface with ApoE was realized by reacting a maleimide group of a PEG-crosslinking agent and thiolated ApoE. *In vitro* studies with an artificial BBB confirmed that NGF remains bioactive after encapsulation and is released from the carrier which induced neurite outgrowth in PC12 cells. The transport of NGF was investigated using a Transwell system and bEnd3 cells, and ApoE-functionalized HSA NPs caused significantly higher NGF levels in the basolateral compartment.<sup>[77]</sup>

In an animal model of stroke (transient middle cerebral artery occlusion model), a combination treatment using NGF-loaded theranostic nanocarriers and the small molecular MEK inhibitor U0126 was tested. A reduction of the infarct volume indicated also an effect of NGF, when using this combinatory therapy, however, no significant difference between this combinatory approach or the use of only U0126 was observed. Consequently, benefits of ApoE-mediated therapy were not clearly perceived.<sup>[77]</sup>

PLGA NPs coated with poloxamer 188 were used to enable the delivery of BDNF (brain-derived neurotrophic factor) into the brain of mice with traumatic brain injury (TBI). BDNF regulates neuronal plasticity, neuronal cell growth, proliferation, cell survival, and long-term memory. The closed head injury weight-drop TBI model was used to induce trauma in mice. BDNF levels were higher after intravenous injection when BDNF was embedded in poloxamer-coated PLGA NPs in comparison to injection of free BDNF and improved neurological and cognitive deficits in TBI mice.<sup>[78]</sup>

For further approaches using peptide- or protein-loaded polymeric NPs for ApoE-mediated brain-targeting see Table 1.

## 5.2. Small Molecules

Brain-delivery of smaller drugs, bound to PBCA NPs, was also tested to study whether transport of dalargin across the BBB with polysorbate-coated PBCA NPs is transferable in a similar way to drugs that completely differ in their chemical structure (Table 2). New drug delivery systems based on small molecules were obtained by encapsulation of, e.g., loperamide, doxorubicin, or tubocurarine into PBCA NPs.<sup>[79]</sup> For tubocurarine-loaded

NPs, used for muscle relaxation, an *in situ* perfused rat brain technique was used together with simultaneous EEG recording as an experimental model. Solely when tubocurarine was embedded in PBCA NPs which were then coated with polysorbate 80, a significant increase in the transport of this drug across the BBB occurred.<sup>[79a]</sup>

As lipophilic and polar drugs, respectively, it was assumed that loperamide and doxorubicin are unable to pass the BBB. Loperamide-loaded particles were obtained by embedding the drug in PBCA NPs, which are then coated with polysorbate 80. Nanoparticles were prepared by emulsion polymerization in the presence of loperamide. The obtained particles were able to cross the BBB after coating with polysorbate 80 shown by induced analgesic effects.<sup>[79b]</sup> Other loperamide-delivery systems were described under Section 4 and in Table 2.

Doxorubicin, as one of the most prominent antitumoral drugs, e.g., for the treatment of glioblastomas,<sup>[80]</sup> is not able to cross the BBB by itself. Therefore, delivery with polysorbate 80-coated PBCA NPs across the intact BBB was studied, and maximum levels after 2 to 4 h after intravenous injection were achieved. The uptake to the brain in comparison to other tissues was a very low, but effective process, whereas administration of free doxorubicin in a polysorbate solution had no effect on brain passage. Thus, nanoparticles are required to mediate transport when they reach the endothelial cells. Doxorubicin levels in spleen, liver, and lung were decreased by about 1.5 times when PBCA NPs were coated with polysorbate. In addition, opening of the tight junctions of the BBB was not detected.<sup>[79c]</sup> Drug distribution in brain tissue after crossing the intact BBB was determined in a subsequent study via a capillary depletion technique to distinguish between amounts of doxorubicin in the whole brain and in the brain parenchyma. Therefore, rats were treated with doxorubicin solutions in polysorbate 80 or doxorubicin-loaded PBCA NPs with and without polysorbate 80 coating via intravenous injection. Clinically effective doxorubicin concentrations in all brain fractions were only found when polysorbate 80-coated PBCA NPs were used indicating significant transcytosis of the drug into the postcapillary parenchymal compartment.<sup>[81]</sup>

The manufacturing parameters of poly(alkylcyanoacrylate) doxorubicin-loaded NPs were optimized regarding surfactants, polymer and doxorubicin-loading using glioblastoma-bearing rats.<sup>[80,82]</sup> Due to the BBB, glioblastomas are nearly inaccessible for commonly used chemotherapeutics. Rats treated with doxorubicin-loaded and polysorbate-coated PBCA NPs showed significantly higher survival times, lower tumor sizes, and lower values for proliferation and apoptosis without showing short-term neurotoxicity.<sup>[80]</sup> The blood half-life of the particles and in turn the uptake due to the so-called enhanced permeability and retention (EPR) effect was also improved by coating with poloxamers/poloxamines instead of polysorbate 80. These surfactants increased the antitumor effect of doxorubicin-loaded PBCA NPs in tumorous brain, but not in healthy brain tissue and across an intact BBB since the permeability of the BBB at the tumor site is significantly increased.<sup>[82,83]</sup> Modifications of variables, such as polymer to surfactant ratio, only led to insignificant effects.<sup>[82]</sup> Poly(iso-hexylcyanoacrylate) (PIHCA) shows a similar efficiency as PBCA for treating cancer in rats, but is better tolerated due to a slightly slower degradation rate. In addition, doxorubicin-loaded PIHCA NPs without surfactant coating are FDA approved

for hepatocellular carcinoma (BioalliancePharma, 2009), but not for brain therapy.<sup>[67b,84]</sup>

Other polymeric NPs such as PS-, PLGA-, and starch-derivatives were investigated as well with regard to transport of doxorubicin for brain targeting across the BBB in vivo, into brain endothelial cells and into glioblastoma cells (Table 2).<sup>[54,85,86]</sup>

Further successfully tested antitumoral drugs used for brain targeting in vivo and in vitro with polysorbate 80-coated PBCA were methotrexate,<sup>[87]</sup> temozolomide,<sup>[88]</sup> and cisplatin.<sup>[89]</sup>

ApoE-functionalization by coating with ApoE was utilized for curcumin transport in PBCA NPs for the potential treatment of cancer and Alzheimer's disease. Curcumin, a natural antioxidant, was hypothesized to inhibit  $\beta$  amyloid and  $\beta$  amyloid induced oxidative stress and shows anticancer activities. For Alzheimer's disease therapy, release of curcumin from ApoE-NPs induced reduction in reactive oxygen species and in  $\beta$  amyloid caused apoptosis in SH-SY5Y neuroblastoma cells. In both disease models, curcumin transport was increased when applying the drug in ApoE-coated PBCA NPs in vitro.<sup>[90]</sup> However, in vivo studies were not performed to validate the findings.

Several other drugs were investigated for Alzheimer's treatment in vivo. Tacrine and rivastigmine-loaded polysorbate 80-coated PBCA NPs were applied to healthy rats, but merely increased brain concentrations were measured.<sup>[91]</sup>

Advanced effects were shown for oral administration of estradiol-loaded polysorbate 80-coated PLGA NPs in an ovariectomized rat model of Alzheimer's disease that mimics the postmenopausal conditions. These NPs provoked a significant increase of estradiol in the brain in comparison to uncoated PLGA NPs. In vitro data in simulated fluids showed that polysorbate 80-coated PLGA NPs were conserved in the gastrointestinal tract transit without loss of coating concentration on the particle. Orally administered estradiol had the same effect as intramuscular drug injection, which simplifies drug administration for patients in post-menopausal Alzheimer's disease.<sup>[92]</sup>

For further approaches using small molecule-loaded polymeric NPs for ApoE-mediated brain-targeting see Table 2.

## 6. In Vitro Blood–Brain Barrier Models

In the field of brain delivery several in vitro blood–brain barrier models have been investigated, which mimic critical functionalities of the BBB and provide first insights in the suitability of a drug delivery system to overcome this barrier. The basic models consist of one type of cells (monoculture), mainly brain endothelial cells of different origin, with which the cellular uptake mechanisms and internalization profiles of the nanocarriers as well as their cytotoxicity and permeability can be assessed. The group of Langer used human brain microvascular endothelial cells (HBMECs) to investigate the uptake of ApoE, penetratin, or ovalbumin modified PLA NPs. Therefore, cells were incubated with different nanoparticle formulations that contained the fluorescent dye Lumogen Red. Cellular uptake was investigated by two methods, first an HPLC-FLD method for quantification, and second, for visualization, a fluorescence microscopy method. In both experiments, the group was able to show increased cellular uptake for ApoE and penetratin (a cell penetrating peptide used as positive control) containing NPs in comparison to unmodified

particles, thus assuming an active targeting of cells by specific interactions between the ApoE ligand and the LRP1 receptor expressed on HBMECs.<sup>[73]</sup>

Primary cerebral endothelial cells (CEC) are frequently used for such in vitro BBB models<sup>[93]</sup> and can be harvested from bovine,<sup>[94]</sup> porcine,<sup>[95]</sup> rat,<sup>[96]</sup> mouse,<sup>[97]</sup> or human<sup>[94]</sup> sources. The advantage of using primary cells is that a large number of cells from one single brain can be isolated and especially the mouse and human endothelial cells provide an important tool for studying the BBB at a cellular and molecular level. However, the isolation process is complex, time consuming and provides cells with high batch-to-batch variability, which leads to low reproducibility of experimental results.<sup>[98]</sup> In order to circumvent these disadvantages of primary cultures, several immortalized CEC lines were created with the potential to provide a stable source with high homogeneity throughout numerous passages.<sup>[99]</sup> These cell lines, from bovine (e.g., BBECS),<sup>[100]</sup> porcine (e.g., PBMECS),<sup>[101]</sup> rat (e.g., RBE4s),<sup>[102]</sup> mouse (e.g., b.End.3s),<sup>[103]</sup> or human (e.g., hCMEC/D3s)<sup>[104]</sup> sources, preserve basic cerebral endothelium-like features, such as tight junction formation, expression of influx, and efflux transporters and endothelial-specific markers. However, immortalized cell lines are generally more permeable than primary cultures.<sup>[104]</sup> One indicator for the tightness of CEC monolayers, and consequently an indirect parameter for the paracellular permeability, is their TEER value, which is evaluated with two voltage-measuring electrodes. The cell layer should display a sufficiently high TEER value to constitute an adequate model system.<sup>[105]</sup> In vitro BBB assays are mostly carried out in multiwell plates, in which compartments simulating the blood (apical) and brain (basolateral) sides are separated by a microporous filter on/under which the cells are seeded. Thus, the cells can develop a monolayer in contact with different culture media in each compartment. In this regard, filters usually include Transwell polycarbonate or polyethylene terephthalate inserts.<sup>[106]</sup> To achieve a better representation of the BBB and to improve barrier functions, coculture and triple coculture systems have been developed (Figure 7). Through the combination of CECs with other elements of the in vivo BBB, i.e., astrocytes, astrocytic cell lines, C6 glioma cell lines, pericytes and/or mixed glia cells, the physiological conditions can be simulated because all compartments of the neurovascular unit strongly contribute to the development and maintenance of the BBB phenotype. In this regard, the second type of cells can either be seeded in close proximity to the endothelial cells at the opposite site of the filter membrane (contact coculture, Figure 7B,D), or without contact at the bottom of the wells (noncontact coculture, Figure 7A,C).<sup>[107]</sup> In triple coculture models, a third cell type of the neurovascular unit is added (triple coculture, Figure 7E,F), that leads, with regard to the stabilization of tight junctions, to a synergistic effect<sup>[108]</sup> and thus, to a higher correlation with in vivo permeability data.<sup>[109]</sup> In these models, higher TEER values can be achieved, if optimal culture conditions parameters are guaranteed.<sup>[73]</sup> The group of Appelt-Menzel recently established a BBB coculture model by using human induced pluripotent stem cells (hiPSC) that advantageously provides a virtually unlimited independent cell source. BBB endothelial cells differentiated from hiPSCs, which are cultured with hiPS-neuronal stem cells and pericytes in a triple culture as well as with astrocytes in a quadruple culture form tight cell layers with TEER

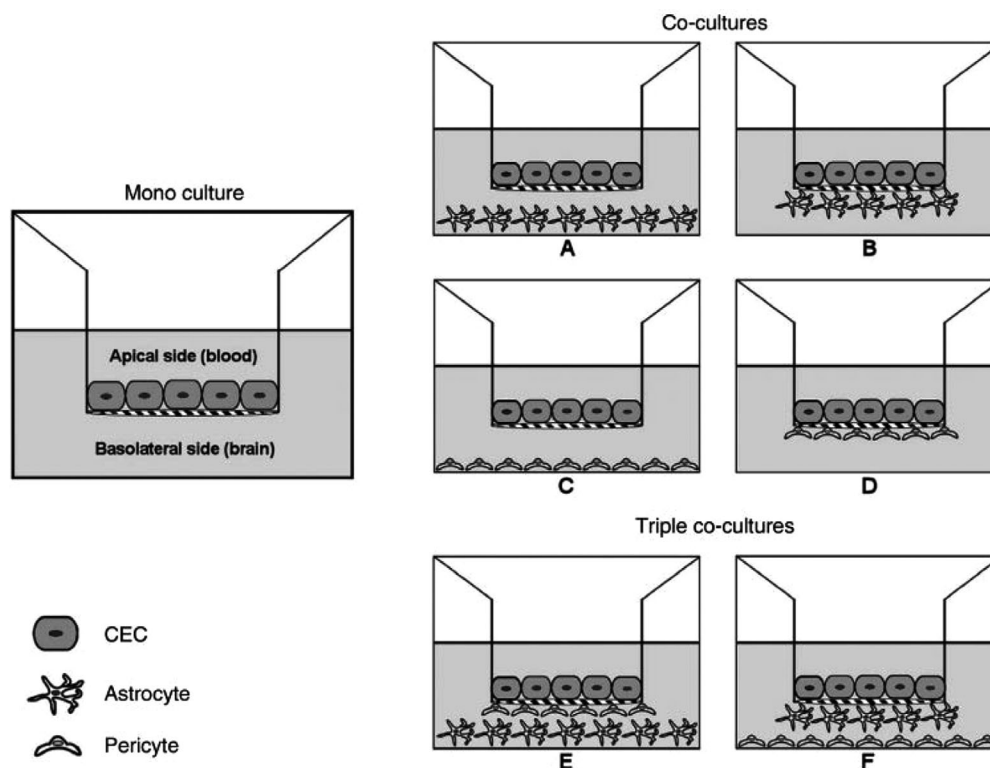


**Figure 7.** Transwell systems to simulate the BBB in vitro. A–D) Mono-, co-, and E,F) triple cocultures of CECs with astrocytes and/or pericytes in B,D) contact or A,C) noncontact set-up. Reproduced with permission.<sup>[98]</sup> Copyright 2014, Elsevier.

values near to physiological conditions. Together with further enhancements in the development of BBB properties this model provides an advanced tool for drug delivery investigations for future approaches.<sup>[140]</sup> For BBB permeability investigations so far, for example, the group of Lee used a Transwell contact coculture model containing a rat brain endothelial cell line (RBE4), which was seeded on the apical side of the filter, and a rat glioma cell line (C6), which was grown on the bottom of the filter. Poloxamer 188- or polysorbate 80-coated PLGA-PEG-PLGA (PEP) NP formulations, containing the centrally analgesic drug loperamide, were added to the apical side and samples from apical and basal compartments were analyzed after an incubation period to quantify the amount of loperamide via HPLC. The group confirmed that surfactant-coated PEP NPs significantly enhanced the permeation percentage compared to unmodified PEP NPs as mandatory tool for BBB penetration.<sup>[55]</sup>

## 7. In Vivo Studies

ApoE-mediated drug delivery across the BBB has been investigated with regard to therapeutic effects in a variety of animal models.

Before assessing therapeutic effects in a model of disease, biodistribution assays (7.1) can lay the ground for therapeutic approaches. Increased delivery into other organs can hinder drugs from reaching their target sites in adequate concentrations and can be solely evaluated in animal models via biodistribution analysis (7.1.1.). To determine the amount of drug that is dis-

tributed within the whole brain, a sophisticated method in case of nanoparticle delivery is capillary depletion (7.1.2.).

As depicted in examples described above, therapeutic cargoes for delivery into the brain have a wide range of effects, which explains the multitude of in vivo models necessary to assess successful delivery to their site of action within the brain. While analgesic drugs need to be studied in pain assessment tests (7.2.), relevant effects of chemotherapeutics can only be determined in cancer models such as glioblastoma models (7.3.). For measuring the effects of anti-AD drug delivery or NGF delivery for the treatment of Parkinson's disease neurodegenerative animal models (7.4.) are required in which histology and behavior as well as potential side effects due to off-target delivery can be tested. The following subsections summarize animal models used in the current literature within the context of either biodistribution profiles (7.1.), pain management (7.2.), brain cancer therapy (7.3.), or neurodegenerative diseases (7.4.), and discuss advantages as well as disadvantages of the models.

### 7.1. Biodistribution Profile Analysis

#### 7.1.1. Body Distribution Analysis

Surfactant-coating of NPs and attachment of ApoE can also lead to LDL receptors-mediated uptake in other organs, such as the RES in which clearance of NPs can occur, specifically described for hepatocytes overexpressing LDL.<sup>[115]</sup> Before assessing therapeutic effects in a model of disease, biodistribution analysis can

lay the ground for therapeutic approaches. Increased delivery into other organs can hinder drugs from reaching their target sites in adequate concentrations and can be solely evaluated in animal models. In the case of AD treatment with tacrine and rivastigmine, Wilson et al. performed body distribution analyses of the drugs in the organs of Wistar rats (brain, liver, lungs, spleen, and kidney) after intravenous injection of nanoparticulate systems and controls via HPLC methods. The results indicated significantly higher tacrine and rivastigmine concentrations in the brain with polysorbate 80-precoated PBCA NPs. However, the group of Wilson reported lower tacrine and rivastigmine accumulation in liver and spleen and higher accumulation in the kidney for polysorbate 80-coated systems, without giving any further explanations or assumptions.<sup>[91]</sup> Kumar and co-workers administered estradiol containing polysorbate 80-PLGA NPs into Sprague–Dawley rats and analyzed the drug concentration after several time points in the brain, small intestine, kidney, spleen, heart, liver, and lung after homogenization with estradiol ELISA kits. The results were in line with previous reports, confirming significantly increased drug levels in the brain after treatment with surfactant-coated NPs in comparison to uncoated NPs. In case of estradiol, accumulation in liver and spleen was found to be reduced as well. The authors therefore suggested that the surfactant coating of NPs alters their surface properties and thus, leads to a lower interaction with cells of the RES and hence to a lower accumulation tendency in RES organs.<sup>[92]</sup> While the techniques used in these experiments detect the actual drug, they are very tedious and require sacrificing sets of animals for each time point. The advantage of image-based biodistribution techniques such as continuous monitoring or various time points in the same animal, however, bear the disadvantage of detecting a label rather than the drug itself.

### 7.1.2. Capillary Depletion Method

To determine the amount of drug that is distributed within the whole brain, a sophisticated method in case of nanoparticle delivery is capillary depletion, which provides the possibility of quantifying the drug that indeed has passed the BBB and appears in the brain parenchyma. For capillary depletion, the brain of treated animals is excised and homogenized in a mortar. After centrifugation, the drug is analyzed in the supernatant which represents the brain parenchyma as well as in the pellet representing the cell debris of vascular elements.<sup>[111]</sup> In a doxorubicin-loaded and polysorbate 80-coated PBCA NP study, the group of Kreuter utilized this method to determine doxorubicin concentrations via HPLC after extraction in different healthy rat brain fractions, whereby whole homogenate, supernatant and pellet represented whole brain, brain parenchyma and brain capillaries, respectively. It was shown, that at one specific time point, the drug concentrations, only when delivered with polysorbate 80-coated NPs, were significantly higher in the supernatant in comparison to the concentrations in the pellet, which indicated a successful transport of the drug across the brain blood capillary endothelium into the brain parenchyma.<sup>[81]</sup> While this bioavailability test did not yet imply therapeutic efficacy, it helped determine optimal time points for further experiments in the disease model.

## 7.2. Pain Assessment Methods

First attempts in brain delivery with ApoE modified NPs were made mainly with centrally analgesic model drugs dalargin and loperamide, a P-glycoprotein substrate. These drugs cause a central analgesic effect, if efficiently delivered into the brain, by binding with  $\mu$ -opioid receptors for pain perception and are expected to be released from drug loaded NPs once they are located in the brain. Hence, central analgesic effects would demonstrate the brain targeting of NPs after administration, since free drugs are not able to pass the BBB.<sup>[52]</sup> To confirm efficient delivery, two established pain assessment methods were utilized.

### 7.2.1. Hot-Plate Test

In general, the hot-plate test is performed by using a water-heated concealed plate that is kept at a constant temperature of  $\approx 55$  °C on which animals are placed. Immediately when they show symptoms of pain perception such as “paw-lick” reaction or jumping, they are removed from the plate. Hot-plate response latencies are measured after several defined incubation times after drug administration. To not further harm animals, a cutoff time is set. The inhibition of the paw-jumping responses due to administration of analgesic drugs is calculated in comparison to the response without treatment and is expressed as the percent of maximum possible effect (MPE).<sup>[110]</sup> In 1998, Schröder and Sabel administered dalargin-loaded polysorbate 80-coated PBCA NPs as well as control formulations intravenously into NMRI mice. Surfactant precoated NPs showed an enhancement over 50% in hot-plate response latency time and therefore improved brain targeting, without being able to state a mechanism at that time.<sup>[44]</sup> In a similar manner, the Lee group reported significantly improved MPE values for loperamide-loaded polysorbate 80-coated PLGA-PEG-PLGA NPs after intravenous injection in ICR mice. However, they also concluded solely that brain targeting with polysorbate 80 was improved without giving any further explanations.<sup>[55]</sup> Lemmer and co-workers reported in a comparable study with dalargin-loaded polysorbate 80-coated PBCA NPs a circadian-phase dependency of NPs transport across the BBB. Therefore, treated mice were subjected to 12 h light-dark cycles and pain reactions were measured by hot-plate test performance. A significant dose-dependent antinociceptive effect was achieved with polysorbate 80-coated NPs which were shifted about 12 h compared to the normal circadian phase-dependent pain reaction of the mice. This result indicated a circadian-time dependent fluctuation in the permeability as well as in the transcytosis capacity of the small cerebral vessels.<sup>[110]</sup> This functional test, however, does not allow for quantitative measurements of bioavailability in the brain, but is one of the established nociception methods available in pain research.

### 7.2.2. Tail-Flick Test

The tail-flick test is conducted with a specific device containing a slit and a quartz projection bulb. The tail of the animal is placed over the slit through which the bulb is focused and the time until the tail is withdrawn is recorded. To prevent tissue damage, the

experiments are terminated after a specific time, if no response was evoked. Tail flick latency is measured after defined incubation times after drug administration and the maximum possible effect (MPE) is calculated in percent. In 2001, Kreuter et al. used the tail-flick test to investigate the brain targeting effect of dalargin-loaded PBCA NPs modified with ApoE with and without polysorbate 80 precoating. The formulations were administered intravenously into ICR mice and MPEs were calculated. It was shown that surfactant precoating additionally to ApoE overcoating achieved significantly higher MPEs in comparison to control groups. Furthermore, polysorbate 80 coating alone demonstrated improved results in comparison to ApoE coating without surfactant. Additionally, tail-flick test results obtained with ApoE-deficient (ApoEtm1Unc) mice demonstrated that ApoE has a crucial role in mediating the delivery of the NPs across the BBB.<sup>[59]</sup> These findings contributed to a better understanding of polysorbate 80 and/or ApoE modified delivery systems to the brain. As discussed above, functional assays cannot estimate bioavailability of the drug in the brain, but need to be put into context of pharmacokinetic/pharmacodynamic (PK/PD) correlation.

### 7.3. Glioblastoma Multiforme Models

Glioblastoma multiforme (GBM) is a devastating type of primary malignant tumor of the CNS that develops from astrocytes. Several GBM in vivo models have been established to investigate the brain delivery and therapeutic effects of anticancer drugs, such as doxorubicin, methotrexate, temozolamide, gemcitabine, cisplatin, carboplatin, curcumin, and docetaxel (Table 2).

#### 7.3.1. 101/8 Glioblastoma Model

The 101/8 glioblastoma rat model is produced by local injection of an  $\alpha$ -dimethylbenzanthracene (DMBA) pellet into the brain of Wistar rats. The developed tumor material is transplanted in new Wistar rat brains. As soon as these animals develop clinical signs, the tumor is removed and inoculated in the brain of further experimental animals. This model was used by Kreuter and co-workers to test the antitumoral effects of doxorubicin-loaded PBCA NPs precoated with different surfactants. After intravenously injection of the formulations, mean survival times of rats were determined and results were shown by Kaplan–Meier plots. Polysorbate 80-coated NPs were shown to be the most effective formulations.<sup>[82]</sup> The same group also utilized this tumor model in another study to investigate the body distribution and BBB permeability using radiolabeled [<sup>14</sup>C]-PBCA NPs. These results showed reduced RES organ concentrations for unloaded polysorbate 80-coated NPs, whereas concentrations of drug loaded polysorbate 80-coated NPs were similar to drug loaded, but uncoated NPs. In addition, it was reported that NP concentrations in the brain of tumor bearing rats were significantly higher compared to concentrations in healthy animals. An experiment with Evans Blue, a dye commonly used to demonstrate a defective BBB, confirmed that the permeability of the BBB in tumor bearing rats is significantly increased after several days due to tumor development, which is described by the EPR effect. Therefore, the authors concluded, that besides the ability of

polysorbate 80-coated NPs to cross the BBB, also the EPR effect plays an important role regarding the capability of nanocarriers to reach a tumorous brain.<sup>[83]</sup> This approach combined drug bioavailability in the brain, biodistribution to assess potential side effects and histological observations to explain the observed results. Considering the principles of the 3Rs (replacement, reduction, and refinement), such experiments ideally reduce the amount of animals necessary in a study. However, for such refined models, often preliminary experiments are necessary to determine optimal time points, drug doses and other parameters.

#### 7.3.2. C6 Brain Tumor Model

The C6 brain tumor model is obtained by an intracerebral C6 murine glioma cell inoculation into the brain of rats.<sup>[112]</sup> The resulting model was utilized by the group of Akbarzadeh in a cisplatin-loaded polysorbate 80-coated PBCA NP approach. After animal treatment with different formulations, the antitumor efficacy was investigated by measuring mean survival times. None of the formulations significantly improved survival times in comparison to the control.<sup>[89]</sup> The group used merely free drug as control, which made the interpretation of the results rather difficult. However, Wang and Chen reported that rats treated with gemcitabine-loaded and polysorbate 80-coated PBCA NPs survived for a significantly longer time than those in the control group by using the same brain tumor model.<sup>[113]</sup>

### 7.4. Neurodegenerative Disease Models

Alzheimer's disease is a progressive neurodegenerative disorder and is characterized by cerebral deposition of beta-amyloid peptides (A $\beta$ ) as amyloid plaques, which are generated by proteolytic processing of the amyloid precursor protein (APP). The major symptoms include a variety of behavioral disturbances and neuropsychiatric symptoms, such as personality change, intellectual debility, and dementia.<sup>[91b]</sup> So far, several anti-AD drugs have been delivered into the brain with nanoparticulate systems, such as tacrine, rivastigmine, estradiol, and rosmarinic acid in preclinical studies (Table 2). Parkinson's disease is caused by a neurodegenerative process with degeneration of dopamine-containing neurons of the nigrostriatal bundle which leads to deficiencies in the motor system, such as bradykinesia, muscular rigidity and tremor and in a later stage of the disease to behavioral problems, dementia, depression, and anxiety. As therapeutic drug, NGF, which is known to prevent degeneration of dopaminergic neurons, has been delivered to the brain via NP formulations preclinically.<sup>[75]</sup> While plaque formation can be best assessed in histologic specimen, the detection of whole body biodistribution provides information about brain bioavailability and potential side effects, and numerous behavioral assays are available to determine pharmacodynamics.

#### 7.4.1. Alzheimer's Disease Rat Model

An AD rat model was established facilitating the analysis of the change in A $\beta$  plaque accumulation in the brain in a physiological



environment and therefore the effect of e.g., rosmarinic acid which is known to reduce amyloid  $\beta$  aggregation.<sup>[114]</sup> The rat model is obtained by injecting  $A\beta_{1-42}$  peptides in the fixed brain of Wistar rats, stitching up the cut in the scalp and observing the rat for one further week. Kuo and Rajesh utilized such an AD model in a study with rosmarinic acid-loaded, ApoE-modified PAAM-CH-PLGA NPs. Nanoparticulate formulations and control formulations were administered intravenously three times every 2 d, then the hippocampus of the rats was removed and sectioned using a cryostat microtome. To visualize  $A\beta$  plaques, samples were treated with an anti- $A\beta$  monoclonal antibody and a goat anti-rabbit immunoglobulin G antibody, coupled with horseradish peroxidase (HRP) and reacted with a common substrate for HRP. Images of stained  $A\beta$  plaques within the samples were acquired with an inverted microscope and showed that the amount of  $A\beta$  plaques in samples treated with ApoE modified NPs were lower in comparison to controls.<sup>[61]</sup> The advantage of such invasive histology-based experiments clearly is the need for additional sets of animals for each time point to be determined at fixed endpoints.

#### 7.4.2. Passive Avoidance Reflex Test

In this passive avoidance reflex test in an induced amnesia mouse model, healthy mice are placed in a two-chamber cage on the side, which is brightly illuminated, whereas the other side is dark. To avoid the light, mice rapidly move into the dark side, where they are exposed to an electric shock.<sup>[116]</sup> After one week of training, the latency time of the animals of remaining on the lighted side is expanded. After induced amnesia in these mice through subcutaneous injection of scopolamine, the animals forget what they have learned and return to basic latency times. Kreuter and co-workers administered NGF-loaded polysorbate 80-coated PBCA NPs into amnesia mice and reported a total reverse of the scopolamine-induced amnesia and even improved recognition and memory.<sup>[76]</sup> As in functional assays described above, this test allows for the assessment of pharmacodynamics, but does not allow for detection of actual drug levels in the brain.

#### 7.4.3. Open-Field Test in Parkinson's Disease Mice Model

In the open-field test, mice are placed in the center of a locomotor activity arena and are allowed to move freely for a certain time in which activity is monitored by an automated video tracking system and behavioral parameters, such as locomotor activity, hyperactivity and exploratory pattern are observed. The group of Kreuter used mice with methylphenyl tetrahydropyridine (MPTP)-induced parkinsonian symptoms for this test, characterized by reduction in the quantity and quality of spontaneous movements (oligokinesia). The degree of oligokinesia was estimated by alteration in locomotor activity of the mice tested by open-field test. Administration of NGF-loaded polysorbate 80-coated PBCA NPs yielded a significant reduction of the main extrapyramidal symptoms compared to control groups and verified therapeutic promise of designed nanocarrier system for Parkinson's disease.<sup>[76]</sup> Also this test can be used to complement

biodistribution and pharmacokinetic assays, but itself does not provide quantitative information about drug levels in the brain.

## 8. Conclusion

Because the BBB is composed of brain microvessel endothelial cells, tight junctions, pericytes, and astrocytes, which all together build a tight cellular barrier, therapeutic (macro)molecules are not able to transit through the BBB by themselves, limiting therapeutic approaches of drugs for brain diseases. CNS diseases are versatile, e.g., depression, epilepsy, Parkinson's disease, dementia/Alzheimer's disease, stroke, or brain tumors, and would require efficient therapeutic agents. Polymeric NPs, consisting of low-cost, tailored, and biodegradable materials have been studied for their suitability as drug delivery tools to the brain. A very efficient way to target the brain was achieved by coating these drug-loaded NPs with surfactants, leading to adsorption of specific proteins on the particle's surface from blood plasma. Thereupon, prolonged circulation time in the blood stream, induced by steric repulsion, led to inhibition/reduction of adsorption onto surfaces of macrophages and thus to a lower particle concentration in organs and tissues belonging to the RES, especially in the liver. Significantly higher levels in the blood and non-RES organs were achieved. In addition, these surfactant-decorated NPs facilitate ApoE anchoring enabling recognition by LDL receptors of brain endothelial cells and can subsequently transit the BBB via receptor-mediated transcytosis. PBCA NPs coated with polysorbate 80 facilitate the brain delivery of a number of drugs that are unable to cross the BBB in free form. Intensive studies were performed with the analgesic drugs dalargin (peptide) and loperamide (small molecule) as well as with the anticancer drug doxorubicin. Several in vitro BBB models were investigated using mono and cocultures of brain endothelial cells with astrocytes/pericytes or glioma cells, which mimic critical functionalities of the BBB and provide first insights in the suitability of a drug delivery system to pass through this barrier. In vivo models were developed with modified rats and mice models to simulate various CNS-relevant diseases such as Alzheimer's disease, Parkinson's disease, cerebral cancer, or stroke. Subsequently, polysorbate 80 was considered as the "gold standard" for brain delivery, but also poloxamer 188 showed high potential when coated onto PLGA NPs. Direct coating of ApoE onto PLGA or PBCA NPs further enhanced the efficiency of brain targeting by RMT. Alternatively, PEG-PHDCAs are able to cross the BBB due to an in vivo long-circulating/stealth effect and adsorption of significant amounts of ApoE on PEG-PHDCAs NPs.

Covalent coupling of ApoE to nanoparticles, via avidin/biotin interaction or direct conjugation, was first enabled by the use of HSA NPs, because these specific types of NPs bear reactive groups on their surfaces. These ApoE-NP complexes led to significantly improved brain uptake without using surfactants. Over the past decades, polymeric NPs have been investigated since they deliver not only small molecule therapeutics, but also proteins and diagnostic agents. These NPs are highly promising drug delivery systems for macromolecules and small molecules in the field of CNS diseases due to their ability to protect the drug during blood circulation and guide them to an appropriate receptor without damaging the BBB. However, to the best

of our knowledge, none of these described formulations using the ApoE-approach are on the market until today, partially because these investigations so far sparked only little interest in the pharmaceutical industry. It will be up to programs such as the BRAIN initiative to translate preclinical findings into medicines.

## Acknowledgements

N.H. and F.A. contributed equally to this work. The authors are thankful for funding by ELSE KRÖNER-FRESENIUS-STIFTUNG, grant number 2014\_A299. This work was supported by the ERC Starting Grant ERC-2014-StG e 637830.

## Conflict of Interest

The authors declare no conflict of interest.

## Keywords

apolipoprotein E, blood–brain barrier, brain targeting, drug delivery, polymeric nanoparticles

Received: April 28, 2020

Revised: July 6, 2020

Published online: July 26, 2020

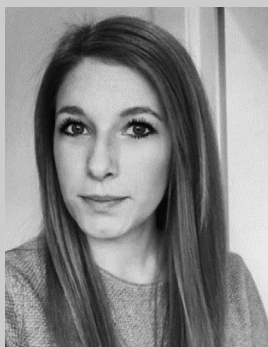
- [1] W. M. Pardridge, *NeuroRx* **2005**, *2*, 3.
- [2] O. van Tellingen, B. Yetkin-Arik, M. C. de Gooijer, P. Wesseling, T. Wurdinger, H. E. de Vries, *Drug Resist. Updates* **2015**, *19*, 1.
- [3] Y.-L. Kwong, D. Y. M. Yeung, J. C. W. Chan, *Ann. Hematol.* **2008**, *88*, 193.
- [4] K. Dorovini-Zis, P. D. Bowman, A. Lorris Betz, G. W. Goldstein, *Brain Res.* **1984**, *302*, 383.
- [5] a) K. Jahnke, D. F. Kraemer, K. R. Knight, D. Fortin, S. Bell, N. D. Doolittle, L. L. Muldoon, E. A. Neuwelt, *Cancer* **2008**, *112*, 581; b) P. J. Robinson, S. I. Rapoport, *J. Cereb. Blood Flow Metab.* **1990**, *10*, 153.
- [6] L. H. Treat, N. McDannold, N. Vykhodtseva, Y. Zhang, K. Tam, K. Hynynen, *Int. J. Cancer* **2007**, *121*, 901.
- [7] A. H. Schinkel, J. J. M. Smit, O. van Tellingen, J. H. Beijnen, E. Wagenaar, L. van Deemter, C. A. A. M. Mol, M. A. van der Valk, E. C. Robanus-Maandag, H. P. J. te Riele, A. J. M. Berns, P. Borst, *Cell* **1994**, *77*, 491.
- [8] Y. Chen, L. Liu, *Adv. Drug Delivery Rev.* **2012**, *64*, 640.
- [9] J. Huwyler, W. M. Pardridge, *J. Neurochem.* **1998**, *70*, 883.
- [10] A. Cerletti, J. Drewe, G. Fricker, A. Eberle, J. Huwyler, *J. Drug Targeting* **2000**, *8*, 435.
- [11] a) N. S. Chung, K. M. Wasan, *Adv. Drug Delivery Rev.* **2004**, *56*, 1315; b) S. Ito, S. Ohtsuki, T. Terasaki, *Neurosci. Res.* **2006**, *56*, 246; c) M. Shibata, S. Yamada, S. R. Kumar, M. Calero, J. Bading, B. Frangione, D. M. Holtzman, C. A. Miller, D. K. Strickland, J. Ghiso, B. V. Zlokovic, *J. Clin. Invest.* **2000**, *106*, 1489; d) P. Candela, J. Saint-Pol, M. Kuntz, M.-C. Boucau, Y. Lamartiniere, F. Gosselet, L. Fenart, *Brain Res.* **2015**, *1594*, 15.
- [12] C. G. Davis, J. L. Goldstein, T. C. Südhof, R. G. W. Anderson, D. W. Russell, M. S. Brown, *Nature* **1987**, *326*, 760.
- [13] P. Ramge, R. E. Unger, J. B. Oltrogge, D. Zenker, D. Begley, J. Kreuter, H. Von Briesen, *Eur. J. Neurosci.* **2000**, *12*, 1931.
- [14] S. Bhaskar, F. Tian, T. Stoeger, W. Kreyling, J. M. de la Fuente, V. Grazú, P. Borm, G. Estrada, V. Ntziachristos, D. Razansky, *Part. Fibre Toxicol.* **2010**, *7*, 3.
- [15] P. Ballabh, A. Braun, M. Nedergaard, *Neurobiol. Dis.* **2004**, *16*, 1.
- [16] D. J. Begley, *J. Pharm. Pharmacol.* **1996**, *48*, 136.
- [17] M. Aurrand-Lions, C. Johnson-Leger, C. Wong, L. Du Pasquier, B. A. Imhof, *Blood* **2001**, *98*, 3699.
- [18] W. M. Pardridge, *J. Cereb. Blood Flow Metab.* **2012**, *32*, 1959.
- [19] N. J. Abbott, A. A. K. Patabendige, D. E. M. Dolman, S. R. Yusof, D. J. Begley, *Neurobiol. Dis.* **2010**, *37*, 13.
- [20] W. Löscher, H. Potschka, *Prog. Neurobiol.* **2005**, *76*, 22.
- [21] S. Gupta, S. Dhanda, R. Sandhir, in *Brain Targeted Drug Delivery System* (Eds: H. Gao, X. Gao), Academic Press, San Diego, CA **2019**, pp. 7.
- [22] J. E. Preston, N. Joan Abbott, D. J. Begley, in *Advanced Pharmacology*, Vol. 71, (Ed: T. P. Davis), Academic Press, San Diego, CA **2014**, pp. 147.
- [23] I. Sauer, I. R. Dunay, K. Weisgraber, M. Bienert, M. Dathe, *Biochemistry* **2005**, *44*, 2021.
- [24] R. D. Broadwell, B. J. Balin, M. Salzman, *Proc. Natl. Acad. Sci. USA* **1988**, *85*, 632.
- [25] D. W. Russell, M. S. Brown, J. L. Goldstein, *J. Biol. Chem.* **1989**, *264*, 21682.
- [26] R. W. Mahley, T. L. Innerarity, S. C. Rall, K. H. Weisgraber, *J. Lipid Res.* **1984**, *25*, 1277.
- [27] R. W. Mahley, J. Stanley C. Rall, *Annu. Rev. Genomics Hum. Genet.* **2000**, *1*, 507.
- [28] R. W. Mahley, *Science* **1988**, *240*, 622.
- [29] A. D. Dergunov, *Biochemistry* **2004**, *69*, 720.
- [30] C.-C. Liu, C.-C. Liu, T. Kanekiyo, H. Xu, G. Bu, *Nat. Rev. Neurol.* **2013**, *9*, 106.
- [31] J. Ribalta, J.-C. Vallvé, J. Girona, L. Masana, *Curr. Opin. Clin. Nutr. Metab. Care* **2003**, *6*, 177.
- [32] D. K. Strickland, S. L. Gonias, W. S. Argraves, *Trends Endocrinol. Metab.* **2002**, *13*, 66.
- [33] B. Dehouck, L. Fenart, M.-P. Dehouck, A. Pierce, G. Torpier, R. Cecchelli, *J. Cell Biol.* **1997**, *138*, 877.
- [34] T. Blunk, D. F. Hochstrasser, J.-C. Sanchez, B. W. Müller, R. H. Müller, *Electrophoresis* **1993**, *14*, 1382.
- [35] M. Lück, B.-R. Paulke, W. Schröder, T. Blunk, R. H. Müller, *J. Biomed. Mater. Res.* **1998**, *39*, 478.
- [36] a) L. Illum, S. S. Davis, *FEBS Lett.* **1984**, *167*, 79; b) L. Illum, S. S. Davis, R. H. Müller, E. Mak, P. West, *Life Sci.* **1987**, *40*, 367.
- [37] S. D. Tröster, U. Müller, J. Kreuter, *Int. J. Pharm.* **1990**, *61*, 85.
- [38] J. Kreuter, U. Täuber, V. Illi, *J. Pharm. Sci.* **1979**, *68*, 1443.
- [39] G. Borchard, K. L. Audus, F. Shi, J. Kreuter, *Int. J. Pharm.* **1994**, *110*, 29.
- [40] S. D. Tröster, J. Kreuter, *Int. J. Pharm.* **1988**, *45*, 91.
- [41] V. Lenaerts, P. Couvreur, D. Christiaens-Leyh, E. Joiris, M. Roland, B. Rollman, P. Speiser, *Biomaterials* **1984**, *5*, 65.
- [42] a) G. Tosi, L. Costantino, B. Ruozi, F. Forni, M. A. Vandelli, *Expert Opin. Drug Delivery* **2008**, *5*, 155; b) N. Voigt, P. Henrich-Noack, S. Kockentiedt, W. Hintz, J. Tomas, B. A. Sabel, *J. Nanopart. Res.* **2014**, *16*, 2379; c) A. M. Hall, R. Hemmer, R. Spaulding, H. N. Wetzel, J. Curcio, B. A. Sabel, P. Henrich-Noack, S. Pixley, T. Hopkins, R. L. Boyce, P. J. Schultheis, K. L. Haik, *J. Drug Targeting* **2016**, *24*, 635.
- [43] J. Kreuter, R. N. Alyautdin, D. A. Kharkevich, A. A. Ivanov, *Brain Res.* **1995**, *674*, 171.
- [44] U. Schröder, B. A. Sabel, *Brain Res.* **1996**, *710*, 121.
- [45] R. N. Alyautdin, A. Reichel, R. Löbenberg, P. Ramge, J. Kreuter, D. J. Begley, *J. Drug Targeting* **2001**, *9*, 209.
- [46] J. Kreuter, V. E. Petrov, D. A. Kharkevich, R. N. Alyautdin, *J. Controlled Release* **1997**, *49*, 81.
- [47] U. Schroeder, H. Schroeder, B. A. Sabel, *Life Sci.* **2000**, *66*, 495.

- [48] R. Rempe, S. Cramer, S. Huwel, H. J. Galla, *Biochem. Biophys. Res. Commun.* **2011**, *406*, 64.
- [49] J.-C. Olivier, L. Fenart, R. Chauvet, C. Pariat, R. Cecchelli, W. Couet, *Pharm. Res.* **1999**, *16*, 1836.
- [50] J. Kreuter, P. Ramge, V. Petrov, S. Hamm, S. E. Gelperina, B. Engelhardt, R. Alyautdin, H. von Briesen, D. J. Begley, *Pharm. Res.* **2003**, *20*, 409.
- [51] U. Schroeder, P. Sommerfeld, B. A. Sabel, *Peptides* **1998**, *19*, 777.
- [52] D. Das, S. Lin, *J. Pharm. Sci.* **2005**, *94*, 1343.
- [53] a) L. Costantino, F. Gandolfi, G. Tosi, F. Rivasi, M. A. Vandelli, F. Forni, *J. Controlled Release* **2005**, *108*, 84; b) G. Tosi, L. Costantino, F. Rivasi, B. Ruozi, E. Leo, A. V. Vergoni, R. Tacchi, A. Bertolini, M. A. Vandelli, F. Forni, *J. Controlled Release* **2007**, *122*, 1.
- [54] S. Gelperina, O. Maksimenko, A. Khalansky, L. Vanchugova, E. Shipulo, K. Abbasova, R. Berdiev, S. Wohlfart, N. Chepurnova, J. Kreuter, *Eur. J. Pharm. Biopharm.* **2010**, *74*, 157.
- [55] Y. C. Chen, W. Y. Hsieh, W. F. Lee, D. T. Zeng, *J. Biomater. Appl.* **2013**, *27*, 909.
- [56] G. Omarch, Y. Kippie, S. Mentor, N. Ebrahim, D. Fisher, G. Murilla, H. Swai, A. Dube, *Artif. Cells, Nanomed., Biotechnol.* **2019**, *47*, 1428.
- [57] Y. Huang, B. Zhang, S. Xie, B. Yang, Q. Xu, J. Tan, *ACS Appl. Mater. Interfaces* **2016**, *8*, 11336.
- [58] S. D. Kong, J. Lee, S. Ramachandran, B. P. Eliceiri, V. I. Shubayev, R. Lal, S. Jin, *J. Controlled Release* **2012**, *164*, 49.
- [59] J. Kreuter, D. Shamenkov, V. Petrov, P. Ramge, K. Cychutek, C. Koch-Brandt, R. Alyautdin, *J. Drug Targeting* **2002**, *10*, 317.
- [60] D. A. Shamenkov, V. E. Petrov, R. N. Alyautdin, *Bull. Exp. Biol. Med.* **2006**, *142*, 703.
- [61] Y. C. Kuo, R. Rajesh, *Int. J. Pharm.* **2017**, *528*, 228.
- [62] M. T. Peracchia, E. Fattal, D. Desmaële, M. Besnard, J. P. Noël, J. M. Gomis, M. Appel, J. d'Angelo, P. Couvreur, *J. Controlled Release* **1999**, *60*, 121.
- [63] M. T. Peracchia, S. Harnisch, H. Pinto-Alphandary, A. Gulik, J. C. Dedieu, D. Desmaële, J. d'Angelo, R. H. Müller, P. Couvreur, *Biomaterials* **1999**, *20*, 1269.
- [64] P. Calvo, B. Gouritin, H. Chacun, D. Desmaële, J. D'Angelo, J.-P. Noël, D. Georgin, E. Fattal, J. P. Andreux, P. Couvreur, *Pharm. Res.* **2001**, *18*, 1157.
- [65] H. R. Kim, K. Andrieux, S. Gil, M. Taverna, H. Chacun, D. Desmaële, F. Taran, D. Georgin, P. Couvreur, *Biomacromolecules* **2007**, *8*, 793.
- [66] H. R. Kim, S. Gil, K. Andrieux, V. Nicolas, M. Appel, H. Chacun, D. Desmaële, F. Taran, D. Georgin, P. Couvreur, *Cell. Mol. Life Sci.* **2007**, *64*, 356.
- [67] a) I. Brigger, J. Morizet, L. Laudani, G. Aubert, M. Appel, V. Velasco, M.-J. Terrier-Lacombe, D. Desmaële, J. d'Angelo, P. Couvreur, G. Vassal, *J. Controlled Release* **2004**, *100*, 29; b) J. Kreuter, *Adv. Drug Delivery Rev.* **2014**, *71*, 2.
- [68] K. Michaelis, M. M. Hoffmann, S. Dreis, E. Herbert, R. N. Alyautdin, M. Michaelis, J. Kreuter, K. Langer, *J. Pharmacol. Exp. Ther.* **2006**, *317*, 1246.
- [69] A. Zensi, D. Begley, C. Pontikis, C. Legros, L. Mihoreanu, S. Wagner, C. Büchel, H. von Briesen, J. Kreuter, *J. Controlled Release* **2009**, *137*, 78.
- [70] S. Wagner, A. Zensi, S. L. Wien, S. E. Tschickardt, W. Maier, T. Vogel, F. Worek, C. U. Pietrzik, J. Kreuter, H. von Briesen, *PLoS One* **2012**, *7*, e32568.
- [71] J. Kreuter, T. Hekmatara, S. Dreis, T. Vogel, S. Gelperina, K. Langer, *J. Controlled Release* **2007**, *118*, 54.
- [72] a) C. Portioli, M. Bovi, D. Benati, M. Donini, M. Perduca, A. Romeo, S. Dusi, H. L. Monaco, M. Bentivoglio, *J. Biomed. Mater. Res.* **2017**, *105*, 847; b) F. Re, I. Cambianica, S. Sesana, E. Salvati, A. Cagnotto, M. Salmona, P.-O. Couraud, S. M. Moghimi, M. Masserini, G. Sancini, *J. Biotechnol.* **2011**, *156*, 341; c) F. Re, I. Cambianica, C. Zona, S. Sesana, M. Gregori, R. Rigolio, B. La Ferla, F. Nicotra, G. Forloni, A. Cagnotto, M. Salmona, M. Masserini, G. Sancini, *Nanomed. Nanotechnol. Biol. Med.* **2011**, *7*, 551.
- [73] B. Raudszus, D. Mulac, K. Langer, *Int. J. Pharm.* **2018**, *536*, 211.
- [74] U. Schroeder, P. Sommerfeld, S. Ulrich, B. A. Sabel, *J. Pharm. Sci.* **1998**, *87*, 1305.
- [75] K. B. Kurakhmaeva, T. A. Voronina, I. G. Kapica, J. Kreuter, L. N. Nerobkova, S. B. Seredenin, V. Y. Balabanian, R. N. Alyautdin, *Bull. Exp. Biol. Med.* **2008**, *145*, 259.
- [76] K. B. Kurakhmaeva, I. A. Djindjikhshvili, V. E. Petrov, V. U. Balabanyan, T. A. Voronina, S. S. Trofimov, J. Kreuter, S. Gelperina, D. Begley, R. N. Alyautdin, *J. Drug Targeting* **2009**, *17*, 564.
- [77] T. Feczko, A. Piiper, S. Ansar, F. W. Blixt, M. Ashtikar, S. Schiffmann, T. Ulshofer, M. J. Parnham, Y. Harel, L. L. Israel, J. P. Lellouche, M. G. Wacker, *J. Controlled Release* **2019**, *293*, 63.
- [78] I. Khalin, R. Alyautdin, T. W. Wong, J. Gnanou, G. Kocherga, J. Kreuter, *Drug Delivery* **2016**, *23*, 3520.
- [79] a) R. N. Alyautdin, E. B. Tezikov, P. Ramge, D. A. Kharkevich, D. J. Begley, J. Kreuter, *J. Microencapsulation* **1998**, *15*, 67; b) R. N. Alyautdin, V. E. Petrov, K. Langer, A. Berthold, D. A. Kharkevich, J. Kreuter, *Pharm. Res.* **1997**, *14*, 325; c) A. E. Gulyaev, S. E. Gelperina, I. N. Skidan, A. S. Antropov, G. Y. Kivman, J. Kreuter, *Pharm. Res.* **1999**, *16*, 1564.
- [80] S. C. J. Steiniger, J. Kreuter, A. S. Khalansky, I. N. Skidan, A. I. Bobruskin, Z. S. Smirnova, S. E. Severin, R. Uhl, M. Kock, K. D. Geiger, S. E. Gelperina, *Int. J. Cancer* **2004**, *109*, 759.
- [81] S. Wohlfart, A. S. Khalansky, S. Gelperina, D. Begley, J. Kreuter, *J. Controlled Release* **2011**, *154*, 103.
- [82] A. Ambruosi, S. Gelperina, A. Khalansky, S. Tanski, A. Theisen, J. Kreuter, *J. Microencapsulation* **2006**, *23*, 582.
- [83] A. Ambruosi, A. S. Khalansky, H. Yamamoto, S. E. Gelperina, D. J. Begley, J. Kreuter, *J. Drug Targeting* **2006**, *14*, 97.
- [84] M. Wacker, *Int. J. Pharm.* **2013**, *457*, 50.
- [85] Y. Malinovskaya, P. Melnikov, V. Baklaushev, A. Gabashvili, N. Osipova, S. Mantrov, Y. Ermolenko, O. Maksimenko, M. Gorshkova, V. Balabanyan, J. Kreuter, S. Gelperina, *Int. J. Pharm.* **2017**, *524*, 77.
- [86] a) M. Gregori, D. Bertani, E. Cazzaniga, A. Orlando, M. Mauri, A. Bianchi, F. Re, S. Sesana, S. Minniti, M. Francolini, A. Cagnotto, M. Salmona, L. Nardo, D. Salerno, F. Mantegazza, M. Masserini, R. Simonutti, *Macromol. Biosci.* **2015**, *15*, 1687; b) J. Li, P. Cai, A. Shalviri, J. T. Henderson, C. He, W. D. Foltz, P. Prasad, P. M. Brodersen, Y. Chen, R. DaCosta, A. M. Rauth, X. Y. Wu, *ACS Nano* **2014**, *8*, 9925.
- [87] K. Gao, X. Jiang, *Int. J. Pharm.* **2006**, *310*, 213.
- [88] X. H. Tian, X. N. Lin, F. Wei, W. Feng, Z. C. Huang, P. Wang, L. Ren, Y. Diao, *Int. J. Nanomed.* **2011**, *6*, 445.
- [89] H. Ebrahimi Shahmabadi, F. Movahedi, M. Koohi Moftakhari Esfahani, S. E. Alavi, A. Eslamifar, G. Mohammadi Anaraki, A. Akbarzadeh, *Tumor Biol.* **2014**, *35*, 4799.
- [90] a) R. S. Mulik, J. Monkkonen, R. O. Juvonen, K. R. Mahadik, A. R. Paradkar, *Int. J. Pharm.* **2012**, *437*, 29; b) R. S. Mulik, J. Monkkonen, R. O. Juvonen, K. R. Mahadik, A. R. Paradkar, *Mol. Pharmaceutics* **2010**, *7*, 815.
- [91] a) B. Wilson, M. K. Samanta, K. Santhi, K. P. Kumar, N. Paramakrishnan, B. Suresh, *Eur. J. Pharm. Biopharm.* **2008**, *70*, 75; b) B. Wilson, M. K. Samanta, K. Santhi, K. P. Kumar, N. Paramakrishnan, B. Suresh, *Brain Res.* **2008**, *1200*, 159.
- [92] G. Mittal, H. Carswell, R. Brett, S. Currie, M. N. Kumar, *J. Controlled Release* **2011**, *150*, 220.
- [93] S. Lundquist, M. Renftel, *Vasc. Pharmacol.* **2002**, *38*, 355.
- [94] D. Zenker, D. Begley, H. Bratzke, H. Rübsamen-Waigmann, H. von Briesen, *J. Physiol.* **2003**, *551*, 1023.
- [95] A. Patabendige, R. A. Skinner, N. J. Abbott, *Brain Res.* **2013**, *1521*, 1.
- [96] N. Perrière, P. H. Demeuse, E. Garcia, A. Regina, M. Debray, J. P. Andreux, P. Couvreur, J. M. Scherrmann, J. Tamsamani, P. O. Couraud, M. A. Deli, F. Roux, *J. Neurochem.* **2005**, *93*, 279.

- [97] C. Weidenfeller, S. Schrot, A. Zozulya, H.-J. Galla, *Brain Res.* **2005**, 1053, 162.
- [98] J. Bicker, G. Alves, A. Fortuna, A. Falcão, *Eur. J. Pharm. Biopharm.* **2014**, 87, 409.
- [99] T. Yang, K. E. Roder, T. J. Abbruscato, *J. Pharm. Sci.* **2007**, 96, 3196.
- [100] K. Sobue, N. Yamamoto, K. Yoneda, M. E. Hodgson, K. Yamashiro, N. Tsuruoka, T. Tsuda, H. Katsuya, Y. Miura, K. Asai, T. Kato, *Neurosci. Res.* **1999**, 35, 155.
- [101] W. Neuhaus, R. Lauer, S. Oelzant, U. P. Fringeli, G. F. Ecker, C. R. Noe, *J. Biotechnol.* **2006**, 125, 127.
- [102] A. Cestelli, C. Catania, S. D'Agostino, I. Di Liegro, L. Licata, G. Schiera, G. L. Pitarresi, G. Savettieri, V. De Caro, G. Giandalia, L. I. Giannola, *J. Controlled Release* **2001**, 76, 139.
- [103] T. Yang, K. E. Roder, T. J. Abbruscato, *J. Pharm. Sci.* **2007**, 96, 3196.
- [104] E. Urich, S. E. Lazic, J. Molnos, I. Wells, P.-O. Freskgård, *PLoS One* **2012**, 7, e38149.
- [105] S. Nakagawa, M. A. Deli, H. Kawaguchi, T. Shimizudani, T. Shimono, Á. Kittel, K. Tanaka, M. Niwa, *Neurochem. Int.* **2009**, 54, 253.
- [106] Y.-C. Kuo, C.-H. Lu, *Colloids Surf.* **2011**, 86, 225.
- [107] K. C.-K. Malina, I. Cooper, V. I. Teichberg, *Brain Res.* **2009**, 1284, 12.
- [108] G. Schiera, E. Bono, M. P. Raffa, A. Gallo, G. L. Pitarresi, I. Di Liegro, G. Savettieri, *J. Cell. Mol. Med.* **2003**, 7, 165.
- [109] É. Hellinger, S. Veszelka, A. E. Tóth, F. Walter, Á. Kittel, M. L. Bakk, K. Tihanyi, V. Háda, S. Nakagawa, T. Dinh Ha Duy, M. Niwa, M. A. Deli, M. Vastag, *Eur. J. Pharm. Biopharm.* **2012**, 82, 340.
- [110] P. Ramge, J. Kreuter, B. Lemmer, *Chronobiol. Int.* **1999**, 16, 767.
- [111] D. Triguero, J. Buciak, W. M. Pardridge, *J. Neurochem.* **1990**, 54, 1882.
- [112] F. K. Miura, M. J. F. Alves, M. C. Rocha, R. S. Silva, S. M. Oba-Shinjo, M. Uno, C. Colin, M. C. Sogayar, S. K. N. Marie, *Arq. Neuro-Psiquiatr.* **2008**, 66, 238.
- [113] C.-X. Wang, L.-S. Huang, L.-B. Hou, L. Jiang, Z.-T. Yan, Y.-L. Wang, Z.-L. Chen, *Brain Res.* **2009**, 1261, 91.
- [114] T. Hase, S. Shishido, S. Yamamoto, R. Yamashita, H. Nukima, S. Taira, T. Toyoda, K. Abe, T. Hamaguchi, K. Ono, M. Noguchi-Shinohara, M. Yamada, S. Kobayashi, *Sci. Rep.* **2019**, 9, 8711.
- [115] a) D. E. Owens, N. A. Peppas, *Int. J. Pharm.* **2006**, 307, 93; b) J.-H. Kang, R. Toita, M. Murata, *Crit. Rev. Biotechnol.* **2016**, 36, 132.
- [116] V. D. Petkov, A. H. Mosharrof, V. V. Petkov, *Acta Physiol. Pharmacol. Bulg.* **1988**, 14, 3.
- [117] N. J. Abbott, *J. Inherited Metab. Dis.* **2013**, 36, 437.
- [118] Y.-H. Hsieh, C.-Y. Chou, *J. Biomed. Sci.* **2011**, 18, 4.
- [119] a) J. Kreuter, *J. Nanosci. Nanotechnol.* **2004**, 4, 484; b) J. Kreuter, *Int. Congr. Ser.* **2005**, 1277, 85.
- [120] G. David, I. M. Jaba, B. Tamba, C. Bohotin, A. Neamtu, X. Patras, B. C. Simionescu, O. C. Mungiu, *Rev. Roum. Chim.* **2010**, 55, 923.
- [121] H. Liu, J. Ni, R. Wang, *Pharmazie* **2006**, 61, 450.
- [122] T. Schuster, A. Muhlstein, C. Yaghootfam, O. Maksimenko, E. Shipulo, S. Gelperina, J. Kreuter, V. Gieselmann, U. Matzner, *J. Controlled Release* **2017**, 253, 1.
- [123] S. Jose, B. C. Juna, T. A. Cinu, H. Jyoti, N. A. Aleykutty, *Colloids Surf.* **2016**, 142, 307.
- [124] C. He, P. Cai, J. Li, T. Zhang, L. Lin, A. Z. Abbasi, J. T. Henderson, A. M. Rauth, X. Y. Wu, *J. Controlled Release* **2017**, 246, 98.
- [125] Z. Li, J. Zhu, Y. Wang, M. Zhou, D. Li, S. Zheng, C. Luo, H. Zhang, L. Zhong, W. Li, J. Wang, S. Gui, B. Cai, Y. Wang, J. Sun, *Asian J. Pharm.* **2019**. <https://doi.org/10.1016/j.ajps.2019.05.002>
- [126] C. X. Wang, L. S. Huang, L. B. Hou, L. Jiang, Z. T. Yan, Y. L. Wang, Z. L. Chen, *Brain Res.* **2009**, 1261, 91.
- [127] B. A. Abdel-Wahab, M. M. Abdel-Latif, A. A. Abdel-Hafez, *Int. J. Nano Biomater.* **2009**, 2, 360.
- [128] C. Grossi, C. Guccione, B. Isacchi, M. Bergonzi, I. Luccarini, F. Casamenti, A. Bilia, *Planta Med.* **2016**, 83, 382.
- [129] A. Friese, E. Seiller, G. Quack, B. Lorenz, J. Kreuter, *Eur. J. Pharm. Biopharm.* **2000**, 49, 103.
- [130] J. Darius, F. P. Meyer, B. A. Sabel, U. Schroeder, *J. Pharm. Pharmacol.* **2000**, 52, 1043.
- [131] M. Liu, H. Li, G. Luo, Q. Liu, Y. Wang, *Arch. Pharm. Res.* **2008**, 31, 547.
- [132] L.-X. Zhao, A.-C. Liu, S.-W. Yu, Z.-X. Wang, X.-Q. Lin, G.-X. Zhai, Q.-Z. Zhang, *Biol. Pharm. Bull.* **2013**, 36, 1263.
- [133] P. Marcianes, S. Negro, L. García-García, C. Montejo, E. Barcia, A. Fernández-Carballido, *Int. J. Nanomed.* **2017**, 12, 1959.
- [134] N. Xu, J. Gu, Y. Zhu, H. Wen, Q. Ren, J. Chen, *Int. J. Nanomed.* **2011**, 6, 905.
- [135] T. Ren, N. Xu, C. Cao, W. Yuan, X. Yu, J. Chen, J. Ren, *J. Biomater. Sci., Polym. Ed.* **2009**, 20, 1369.
- [136] M. Bagad, Z. A. Khan, *Int. J. Nanomed.* **2015**, 10, 3921.
- [137] Y. C. Kuo, F. L. Su, *Int. J. Pharm.* **2007**, 340, 143.
- [138] S. Wagner, J. Kufleitner, A. Zensi, M. Dadparvar, S. Wien, J. Bungert, T. Vogel, F. Worek, J. Kreuter, H. von Briesen, *PLoS One* **2010**, 5, e14213.
- [139] P. Girotra, S. K. Singh, *Pharm. Res.* **2016**, 33, 1682.
- [140] A. Appelt-Menzel, A. Cubukova, K. Günther, F. Edenhofer, J. Piontek, G. Krause, T. Stüber, H. Walles, W. Neuhaus, M. Metzger, *Stem Cell Rep.* **2017**, 8, 894.



**Natascha Hartl** received her degree in pharmacy from the Ludwig-Maximilians-Universität München, Germany in 2015, following which she worked in a public pharmacy and was recruited as Ph.D. student at the group of Prof. Merkel at the chair of Pharmaceutical Technology and Biopharmacy in 2017. Her research interest focuses on the development of polymeric nanocarrier systems for nucleic acids in the field of targeted drug delivery to the brain.



**Friederike Adams** received her M.Sc. degree in chemistry with a special focus on organic and macromolecular chemistry in 2015 and her Ph.D. degree in polymer chemistry in 2019, both at the Technical University of Munich, Germany. Following her Ph.D., she joined the Ludwig-Maximilians-Universität München, Germany, in 2018, where she is currently a postdoctoral researcher in the group of Prof. Merkel at the chair of Pharmaceutical Technology and Biopharmacy. Her research interest focuses on the design and development of innovative drug delivery systems for low molecular weight drugs and biomacromolecules based on novel polyamide- or polyamine-containing carriers.



**Olivia M. Merkel** received her degree in pharmacy from the Philipps-Universität Marburg, Germany, in 2004, her M.S. in Pharmaceutical Technology from Martin-Luther-Universität Halle-Wittenberg, Germany, in 2006, her Ph.D. in Pharmaceutical Technology from the Philipps-Universität Marburg, Germany, in 2009, and was a postdoctoral associate and lecturer until 2011 when she accepted a Tenure Track Assistant Professorship in Pharmaceutical Sciences at Wayne State University, Detroit, MI. She became Associate Faculty of Oncology at WSU in 2012 and accepted a Professorship for Drug Delivery at Ludwig-Maximilians-Universität München, Germany, in 2015. Her research interests are drug and gene delivery using novel and smart dosage forms with a focus on pulmonary administration.